



FRONTLINE | Research Article

Peripheral and systemic antigens elicit an expandable pool of resident memory CD8⁺ T cells in the bone marrow

Maria Fernanda Pascutti¹, Sulima Geerman¹, Nicholas Collins², Giso Brassler¹, Benjamin Nota^{3,4}, Regina Stark¹, Felix Behr¹, Anna Oja¹, Edith Slot¹, Eleni Panagiotti⁵, Julia E. Prier², Sarah Hickson¹, Monika C. Wolkers¹, Mirjam H.M. Heemskerk⁶, Pleun Hombrink¹, Ramon Arens⁵, Laura K. Mackay², Klaas P.J.M. van Gisbergen¹  and Martijn A. Nolte^{1,3,4} 

¹ Department of Hematopoiesis, Sanquin Research, Amsterdam, The Netherlands

² Department of Microbiology and Immunology, Peter Doherty Institute for Infection and Immunity, The University of Melbourne, Melbourne, Australia

³ Department of Molecular and Cellular Hemostasis, Sanquin Research, Amsterdam, The Netherlands

⁴ Landsteiner Laboratory, Amsterdam UMC, University of Amsterdam, Amsterdam, The Netherlands

⁵ Department of Immunohematology and Blood Transfusion, Leiden University Medical Center, Leiden, The Netherlands

⁶ Department of Hematology, Leiden University Medical Center, Leiden, The Netherlands

BM has been put forward as a major reservoir for memory CD8⁺ T cells. In order to fulfill that function, BM should “store” memory CD8⁺ T cells, which in biological terms would require these “stored” memory cells to be in disequilibrium with the circulatory pool. This issue is a matter of ongoing debate. Here, we unequivocally demonstrate that murine and human BM harbors a population of tissue-resident memory CD8⁺ T (T_{RM}) cells. These cells develop against various pathogens, independently of BM infection or local antigen recognition. BM CD8⁺ T_{RM} cells share a transcriptional program with resident lymphoid cells in other tissues; they are polyfunctional cytokine producers and dependent on IL-15, Blimp-1, and Hobit. CD8⁺ T_{RM} cells reside in the BM parenchyma, but are in close contact with the circulation. Moreover, this pool of resident T cells is not size-restricted and expands upon peripheral antigenic re-challenge. This work extends the role of the BM in the maintenance of CD8⁺ T cell memory to include the preservation of an expandable reservoir of functional, non-recirculating memory CD8⁺ T cells, which develop in response to a large variety of peripheral antigens.

Keywords: bone marrow · infection · CD69 · Hobit · resident memory T cells



See accompanying Commentary by Zens and Münz



Additional supporting information may be found online in the Supporting Information section at the end of the article.

Correspondence: Dr. Martijn A. Nolte and Maria F. Pascutti
e-mail: m.nolte@sanquin.nl; f.pascutti@sanquin.nl

© 2019 The Authors. *European Journal of Immunology* published by WILEY-VCH Verlag GmbH & Co. KGaA, Weinheim.

This is an open access article under the terms of the Creative Commons Attribution-NonCommercial-NoDerivs License, which permits use and distribution in any medium, provided the original work is properly cited, the use is non-commercial and no modifications or adaptations are made.

www.eji-journal.eu

Introduction

Memory CD8⁺ T cells are classically divided into different subsets based on their circulatory patterns: central memory T cells (T_{CM}) patrol secondary lymphoid organs, governed by expression of homing molecules CD62L and CCR7, whereas effector memory T cells (T_{EM}) lack these and express other homing molecules, which enable them to recirculate through nonlymphoid organs [1]. Both CD8⁺ T_{CM} and T_{EM} cells leave the tissues they patrol through blood or lymph by means of CCR7 and/or the sphingosine-1-phosphate receptor (S1PR1), and thereby return to the circulation [1, 2]. In the past decade, a subset of memory T cells has been identified in both lymphoid and nonlymphoid organs that does not recirculate (reviewed in ref. [3, 4]). These tissue-resident memory T (T_{RM}) cells are characterized by the expression of CD69 and the lack of S1PR1 and CCR7, which inhibits their egress through blood or lymph and thereby their ability to recirculate [5]. CD69 is a valid and functional marker for T_{RM} cells, because of its ability to directly inhibit expression of S1PR1 [6], though tissue residency has also been observed in CD69-negative CD8⁺ T cells [7]. CD8⁺ T_{RM} cells are important for local tissue protection, as their reactivation leads them to proliferate and accelerate clearance of local re-infections, independently of the circulatory pool [8, 9]. Moreover, local activation of CD8⁺ T_{RM} cells can also provide protection against unrelated pathogens, as their production of IFN- γ elicits a pro-inflammatory gene expression profile in surrounding tissue cells, which boosts innate immunity and induces the recruitment of circulating CD8⁺ T cells [10, 11].

In recent years, CD8⁺ T_{RM} cells have been found in virtually every tissue. They were first identified in tissues exposed to external pathogens (skin, lungs, intestines, and female reproductive tract), then in internal organs (liver, kidney, and brain), and also in lymphoid organs (lymph nodes, spleen, and thymus; reviewed in ref. [3]). When comparing resident lymphoid cells from different tissues, they were found to share a core transcriptional expression program, which keeps the cells from recirculating and thereby enables them to mediate local immune-surveillance [12, 13]. We found that the transcription factors Blimp-1 and Hobit play an important role in establishing this expression program and thereby in the differentiation of CD8⁺ T_{RM} cells [13].

The BM has been considered an important reservoir for long-term T cell memory [14–16]. In both human and mice, there is an increased frequency of memory T cells compared to secondary lymphoid organs and blood [16–18]. Moreover, when taking its total volume into account, BM contains one of the largest pools of memory CD8⁺ T cells in the body; we recently showed that the total number of virus-specific CD8⁺ memory T cells in the BM is five to six times higher than in the spleen [19]. A preference of memory CD8⁺ T cells for the BM may be driven by the presence of IL-7- and IL-15-expressing stromal cells, which can contribute to their survival and long-term maintenance [14, 17, 20]. But despite its well-established role as a memory organ, the BM has not been included in numerous studies that addressed the presence and function of CD8⁺ T_{RM} cells [3, 7, 13, 21, 22].

Although CD69 is expressed on a subset of BM CD8⁺ T cells [14, 16, 17, 23–25], the total BM memory pool does not appear to be recently activated and CD69⁺ CD8⁺ T cells show some features of residency, such as low S1PR1 expression [17]. In fact, the migratory behavior of BM memory CD8⁺ T cells is still under debate: it has been suggested that the majority of memory CD8⁺ T cells in the BM are recirculating [26], whereas it has also been proposed that a substantial subset of these cells, even the majority, is resident to the BM [16, 17, 19, 27].

To thoroughly investigate whether the BM contains CD8⁺ T_{RM} cells and what their requirements for BM residency would be, we used a variety of different infection, immunization, and adoptive transfer models, including parabiosis experiments. Based on our experiments, we can conclude that the BM harbors a subset of bona fide CD8⁺ T_{RM} cells, next to a pool of conventional circulating memory CD8⁺ T cells. We show that CD69⁺ CD8⁺ T cells in the BM express the transcriptional core program of resident lymphoid cells, on top of a BM-specific gene signature, and we reveal both intrinsic and extrinsic factors required for the generation and/or maintenance of CD8⁺ BM T_{RM} cells. These findings demonstrate that the important role of the BM in maintenance of immunological memory is not only governed by supporting recirculating memory T cells, but also by providing residency to a substantial pool of noncirculating, fully functional memory CD8⁺ T cells that is directed against a large variety of systemic and peripheral antigens.

Results

Memory CD8⁺ T cells with a resident phenotype are present in BM after acute systemic infections

To examine whether the BM develops a pool of resident memory CD8⁺ T cells in response to a systemic viral infection, we infected mice with the Armstrong strain of lymphocytic choriomeningitis virus (LCMV), which is efficiently cleared within 2 weeks. After >150 days, memory CD8⁺ T cells directed against different immunodominant viral epitopes could still be detected in the BM, with similar frequencies as in the spleen (Supporting Information Fig. 1A and Fig. 1A). Yet, we observed that BM from LCMV-infected mice was significantly enriched for virus-specific CD69⁺ CD62L⁻ CD8⁺ T cells compared to the spleen, whereas the fractions of virus-specific CD62L⁺ CD8⁺ T cells (i.e., T_{CM} cells) or CD69⁻ CD62L⁻ (i.e., T_{EM}) CD8⁺ T cells were comparable in both organs (Fig. 1B and C and Supporting Information Fig. 2A and B). Similar results were obtained after systemic acute infection with OVA-expressing *Listeria monocytogenes* (Listeria-OVA, Fig. 1D–F). We observed that both total and LCMV-specific CD69⁺ CD62L⁻ CD8⁺ T cells in the BM expressed significantly higher levels of CXCR3, CXCR6, and lower levels of CX₃CR1 (Fig. 1G–I and Supporting Information Fig. 2C–G), which corresponds to the phenotype of CD8⁺ T_{RM} cells in other murine tissues [28, 29]. These results suggest that systemic infections with an

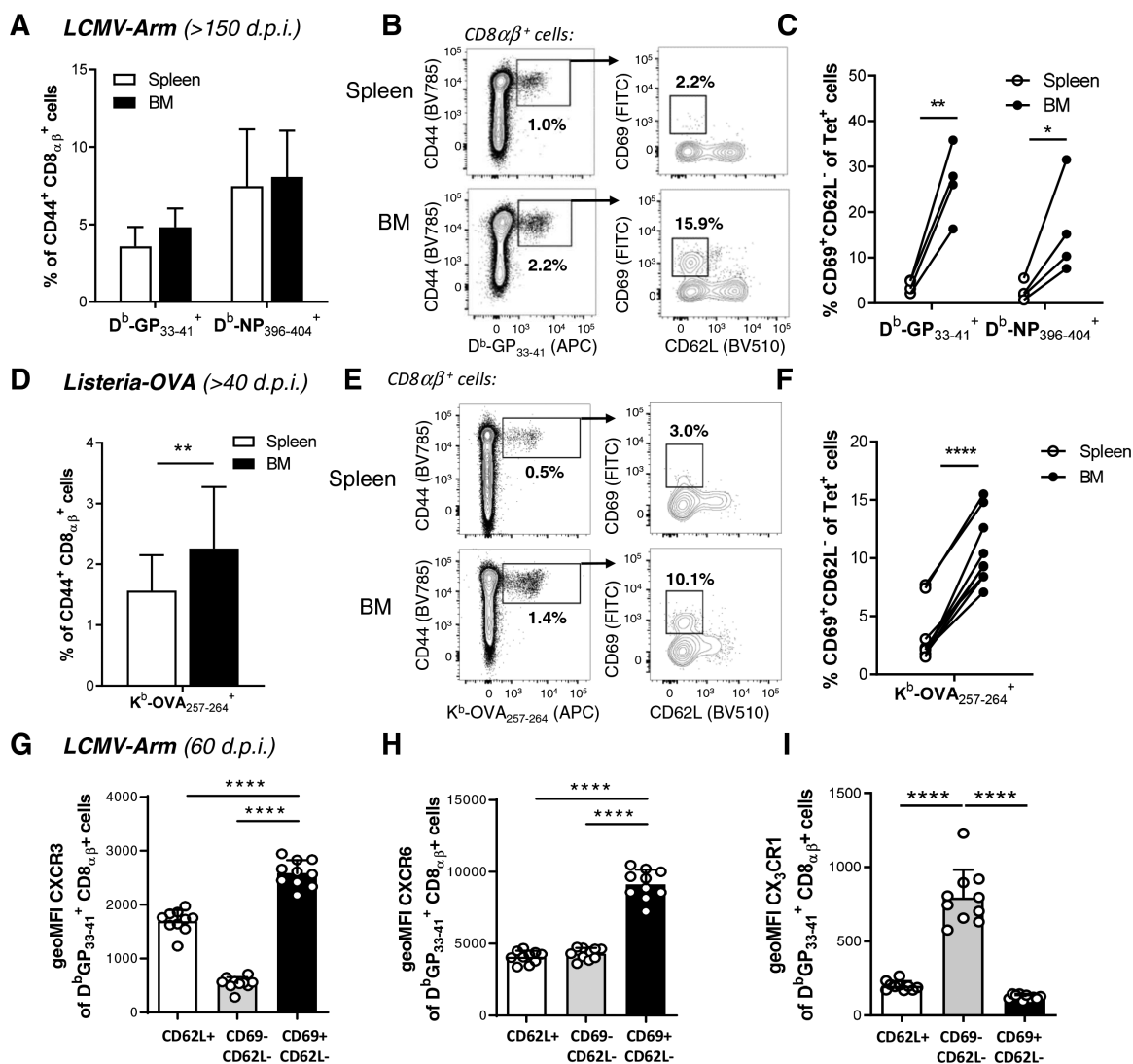


Figure 1. Memory CD8⁺ T cells with a resident phenotype are present in murine BM after acute systemic infection. (A–C) Spleen and BM were analyzed for virus-specific CD8⁺ T cells, 172 days after systemic infection with LCMV Armstrong. Data are shown for one representative experiment with $n = 4$ mice, out of three independent experiments; (A) Frequency of LCMV GP₃₃₋₄₁-specific and NP₃₉₆₋₄₀₄-specific CD8⁺ T cells of all CD44⁺ CD8⁺ T cells (average + SD); (B) Representative FACS staining for CD69 and CD62L on LCMV GP₃₃₋₄₁-specific CD44⁺ CD8⁺ T cells from spleen and BM; (C) Paired analysis for the percentage of CD62L⁻ CD69⁺ cells of all LCMV GP₃₃₋₄₁-specific or NP₃₉₆₋₄₀₄-specific memory CD8⁺ T cells in spleen versus BM. (D–F) Analysis of OVA-specific CD8⁺ T cells in spleen and BM of WT mice, 49 days after systemic infection with *Listeria-OVA*. Data are shown for one representative experiment with $n = 9$ mice, out of two independent experiments; (D) Frequency of OVA₂₅₇₋₂₆₄-specific CD8⁺ T cells of all CD44⁺ CD8⁺ T cells (average + SD); (E) Representative FACS staining for CD69 and CD62L on OVA₂₅₇₋₂₆₄-specific CD44⁺ CD8⁺ T cells from spleen and BM; (F) Paired analysis for the percentage of CD62L⁺ CD69⁺ cells of all OVA₂₅₇₋₂₆₄-specific memory CD8⁺ T cells in spleen vs BM. (G–I) Expression levels of (G) CXCR3, (H) CXCR6, and (I) CX₃CR1 in D^b-GP₃₃₋₄₁-specific memory CD8⁺ T cell subsets in BM, 60 days after systemic infection with LCMV Armstrong. Data are shown for one representative experiment with $n = 10$ mice, out of two independent experiments. Data were analyzed by two-tailed t-test, with matching (D, F), one-way ANOVA followed by Tukey's multiple comparisons test (G–I) and two-way ANOVA, with matching, followed by Bonferroni's multiple comparison test (C). Significance is indicated by * $p < 0.05$; ** $p < 0.01$; and **** $p < 0.0001$.

intracellular pathogen induce the development of specific memory CD8⁺ T cells in the BM with a tissue-resident phenotype.

Generation of CD8⁺ T_{RM} cells does not require local infection or antigen presentation

In nonlymphoid tissues, T_{RM} cell development and maintenance is strongly enhanced by the local recognition of antigen and/or

inflammatory mediators [30, 31]. To test whether development of pathogen-specific, resident-like BM CD8⁺ T cells is dependent on infection of the BM itself, we infected mice with influenza virus, which is restricted to the airways and does not infect BM [32]. Interestingly, in the memory phase (>30 days post infection) we found a significant enrichment of CD69⁺ influenza-specific CD8⁺ T_{EM} cells in BM compared to the spleen (Fig. 2A). Similar observations were made in a local skin-infection model using HSV-1: we found that adoptive transfer of naïve CD45.1⁺ gBT-I CD8⁺

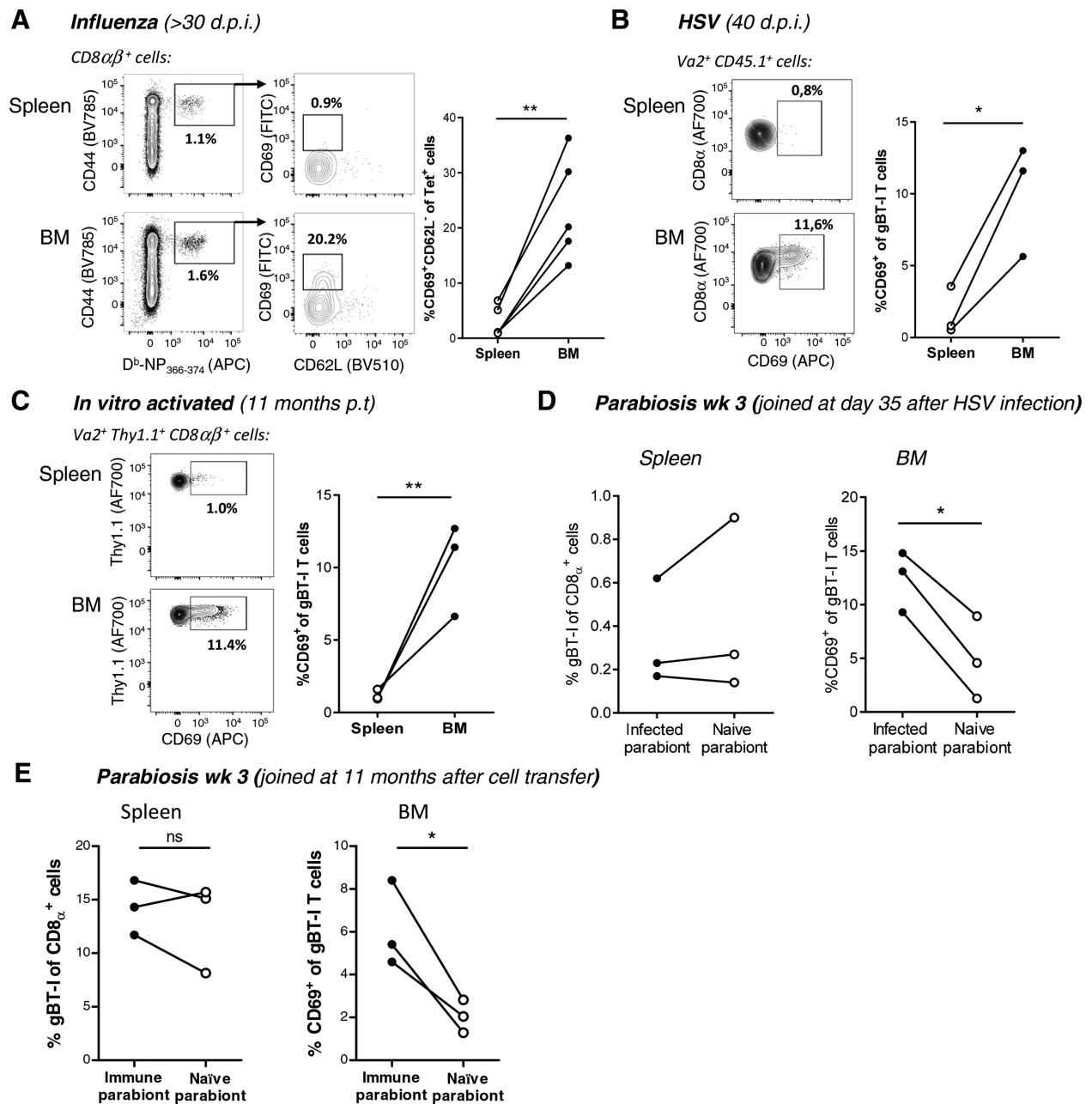


Figure 2. Generation of BM CD8⁺ T_{RM} cells does not require local infection or antigen presentation. (A) Percentage of CD69⁺ CD62L⁻ cells within Influenza NP₃₆₆₋₃₇₄-specific CD44⁺ CD8⁺ T cells in spleen and BM 33 days after intranasal infection with Influenza A/HKx31. Data are shown from one representative experiment with $n = 5$ mice, out of two independent experiments; (B) Naïve WT mice were epicutaneously infected with HSV-1 one day after i.v. transfer of 5×10^4 gBT-I CD8⁺ T cells, which recognize the HSV-1 K^b-gB₄₉₈₋₅₀₅ epitope and are identified as Va2⁺ Thy1.1⁺. Expression of CD69 was analyzed on donor cells in spleen and BM 40 days after infection; (C) Percentage of CD69⁺ within gBT-I CD8⁺ T cells in spleen and BM, 11 months after in vitro activation and transfer; for (B) and (C), experiments were performed twice. (D) Frequency of gBT-I cells within total CD8 α ⁺ cells in the spleen (left) or CD69⁺ within gBT-I cells in the BM (right) of conjoined mice that received gBT-I and were subsequently infected with HSV, as shown in (B); (E) Frequency of gBT-I cells within total CD8 α ⁺ cells in the spleen (left) or CD69⁺ within gBT-I cells in the BM (right) of conjoined mice that received in vitro activated gBT-I cells, as shown in (C). For (D) and (E), organs were analyzed 3 weeks after conjoining. For (D) and (E), data are shown from one experiment with $n = 3$ mice. Data were analyzed by two-tailed t-test, with matching. Significance is indicated by * $p < 0.05$ and ** $p < 0.01$.

T cells (which are transgenic T cells specific for an immunodominant H2-K^b restricted epitope of HSV-1) to CD45.2⁺ recipient mice, followed by skin infection with HSV-1, led to a significant enrichment of CD69⁺ gBT-I cells in the BM compared to spleen

in the memory phase of infection (Supporting Information Fig. 1B and Fig. 2B).

Although the development of pathogen-specific, resident-like BM CD8⁺ T cells is independent of local infection, it is possible

that pathogen-derived antigens are transported to the BM following infection, where they could be presented to CD8⁺ T cells by local DCs [33]. To determine whether local antigen-recognition by CD8⁺ T cells in the BM is required for resident-like memory CD8⁺ T cell development, we transferred in vitro activated gBT-I CD8⁺ T cells into naïve recipient mice. Eleven months after transfer, a stable pool of memory T cells had formed in both spleen and BM, and also in this setting, we observed that the BM was enriched for CD69⁺ gBT-I T cells compared to the spleen (Supporting Information Fig. 1C and Fig. 2C). As the cognate antigen for gBT-I T cells is not present in these mice, these data demonstrate that local antigen recognition is not required for the development of CD8⁺ T_{RM}-like cells in the BM.

Finally, to formally demonstrate the permanent residence of these CD69⁺ memory CD8⁺ T cells in the BM, we performed parabiosis experiments to induce a shared blood circulation [34]. For this purpose, naïve mice (naïve parabionts) were surgically conjoined with mice that had, as shown in Fig. 2B, received naïve gBT-I CD8⁺ T cells and were subsequently skin infected with HSV-1 35 days before surgery (infected parabionts). Three weeks after the conjoining surgery, we found equal numbers of gBT-I memory T cells in spleens of both groups of mice, indicating that their blood circulation was in equilibrium (Fig. 2D, left). However, CD69⁺ gBT-I memory cells remained significantly enriched in the BM of the infected parabionts, compared to their conjoined naïve parabiont (Fig. 2D, right). Moreover, when we performed parabiosis with mice that received in vitro activated gBT-I T cells (as per Fig. 2C) and nontransferred control animals, we observed a similar effect (Fig. 2E). Given that circulatory memory equilibrates in the BM as soon as 2 weeks after conjoining mice [35], we conclude that the BM also harbors a population of bona fide pathogen-specific, tissue-resident memory CD8⁺ T cells. This development is not restricted to a particular route of infection, nor dependent on local antigen-presentation.

Virus-specific resident-like CD8⁺ T cells are found within human BM

Following previous observations that human BM also contains CD69⁺ CD8⁺ T cells with a resting memory phenotype [14, 16, 25], we examined the phenotype of these cells and addressed whether they also contain virus-specific cells. We found that, unlike CD8⁺ T_{RM} cells from epithelial barrier tissues, BM CD69⁺ CD8⁺ T cells were mostly CD103⁻ (Supporting Information Fig. 1D and Fig. 3A), which is also the case in mice (data not shown). Human BM CD69⁺ CD8⁺ T cells also expressed significantly higher levels of CXCR6 and CCR5 and lower levels of CX₃CR1, compared to the CD69⁻ CD8⁺ T cells (Fig. 3B and C), which is in concordance with the CD8⁺ T_{RM} cell phenotype in other human tissues [12], and murine BM (Fig. 1G–I and Supporting Information Fig. 2C–G).

As human BM has a higher frequency of CD4⁺ and CD8⁺ T cells against certain viral epitopes [16, 36], we examined the presence of virus-specific memory CD8⁺ T cells with a resident phenotype. Therefore, we probed human HLA-typed BM samples for the

presence of human cytomegalovirus (CMV)- and EBV-specific CD8⁺ T cells. To ensure that the measurements would be sufficiently sensitive to detect low frequencies of antigen-specific T cells, we used a combinatorial coding approach with MHC-I tetramers [37], loaded with immunodominant epitopes from either CMV or EBV (Table 1). Using this method, we were able to identify a total of 15 virus-specific CD8⁺ T cell populations in five BM samples (Supporting Information Fig. 1E and Fig. 3D and E), with an average of 1.10% CMV-specific CD8⁺ T cells and 0.49% EBV-specific CD8⁺ T cells of total CD8⁺ T cells (Fig. 3F). CD8⁺ T cells specific for either virus contained a subset of CD69⁺ cells (Fig. 3G). These results, therefore, support the hypothesis that human BM also contains virus-specific CD8⁺ T_{RM} cells.

Steady-state BM is enriched for CD69⁺ memory CD8⁺ T cells that share strong homology with T_{RM} cells in other organs

Given that BM CD8⁺ T_{RM} cells develop against a large variety of both systemic and peripheral antigens, we next focused on the broad pool of memory CD8⁺ T cells in the BM of steady-state mice. We found that in naïve animals, the BM contains significantly more CD8⁺ T cells expressing CD44 as compared to those in the spleen or peripheral blood (Fig. 4A), and we found that a substantial fraction of these CD8⁺ CD44⁺ T cells expressed CD69 (Fig. 4B). The expression of CD69 is predominantly found on CD8⁺ T cells with a T_{EM}, rather than a T_{CM} phenotype in the BM, whereas the corresponding memory subsets in spleen and peripheral blood lack CD69 expression (Fig. 4C). Further analysis of the different memory populations within total CD44⁺ pool of CD8⁺ T cells revealed that steady-state BM is significantly enriched for CD69⁺ CD62L⁻ and CD69⁺ CD62L⁺ cells compared to the spleen (Fig. 4D). These results are in agreement with our findings for antigen-specific memory CD8⁺ T cells (Figs. 1 and 2). RT-qPCR analysis revealed that CD69⁺ CD62L⁻ memory (CD44⁺) CD8⁺ T cells in the BM express low levels of *S1pr1*, *Klf2*, and *Ccr7*, and high levels of *Zfp683* (encoding Hobit), which is consistent with their T_{RM} phenotype (Fig. 4E–H). To thoroughly investigate the residency profile of BM T_{RM} cells, we performed genome-wide transcriptional profiling on T_{RM}-like CD8⁺ T cells and compared this to T_{NV}, T_{CM}, and T_{EM} CD8⁺ T cells from steady-state BM. This revealed that only the expression profile from T_{RM}-like BM cells fully mirrors the gene expression program that is associated with tissue residency in various other tissue sites and across immune lineages [13]; 22 of the 30 genes from this program are significantly different from BM T_{EM} and/or T_{CM} (Fig. 4I and Table 2).

Steady-state BM T_{RM} cells are efficient, polyfunctional cytokine producers

The BM has been proposed to act as a “reservoir” for memory T cells [15, 25, 36]. We showed thus far that the BM contains both a circulating (T_{CM} and T_{EM} cells) and a resident memory CD8⁺ T cell

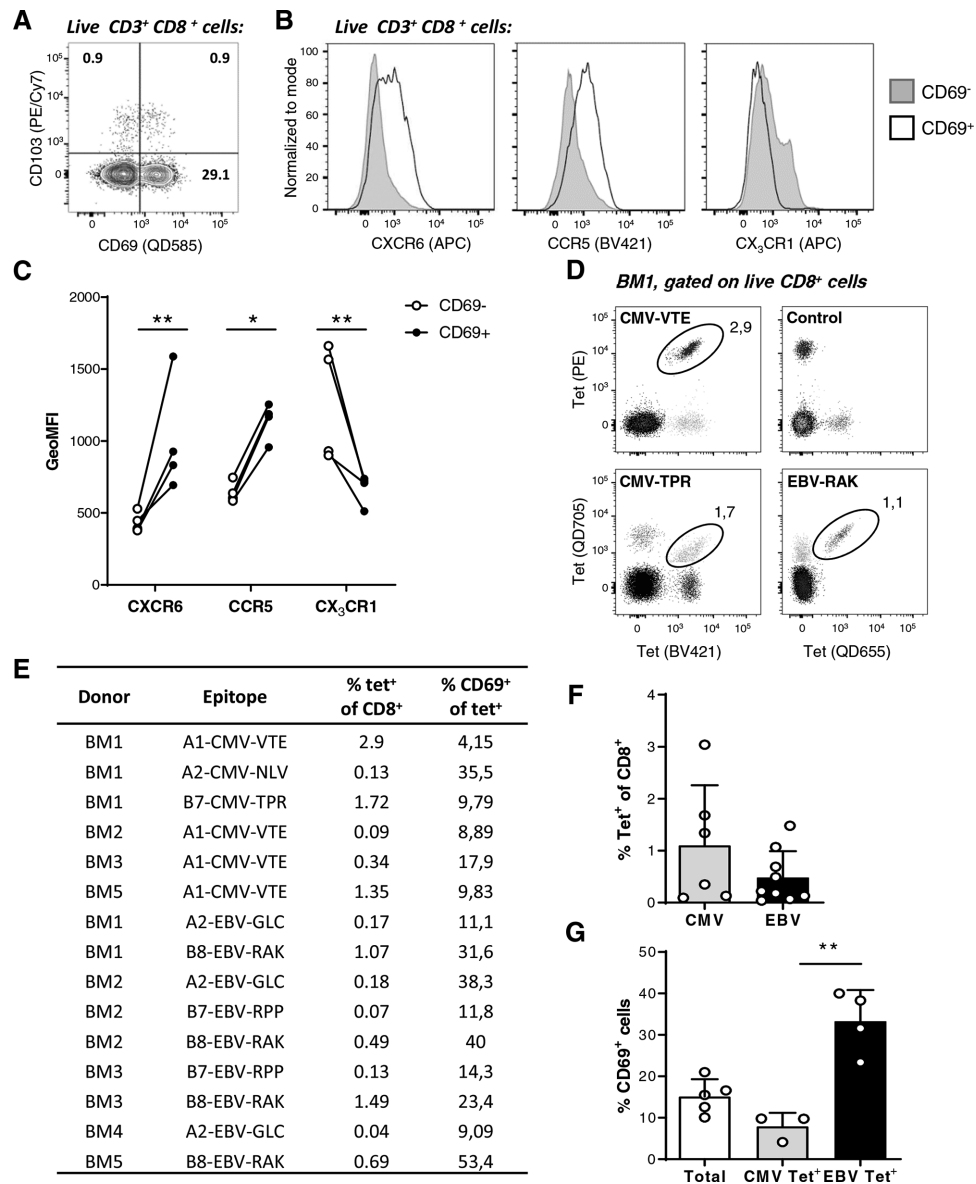


Figure 3. Virus-specific resident-like CD8⁺ T cells are found within human BM. (A) Representative staining for CD69 and CD103 on CD8⁺ CD3⁺ T cells in human BM; (B and C) Expression of chemokine receptors CXCR6, CCR5, and CX₃CR1 on CD69⁻ and CD69⁺ CD8⁺ T cells in human BM; (B) Representative histograms for CD69⁻ and CD69⁺ CD8⁺ T cells; (C) Expression levels depicted as geoMFI for the same populations. For (A–C), data are shown for *n* = 4 non-HLA typed BM samples from four different donors; (D) Combinatorial coding analysis of human CD8⁺ BM T cells specific for CMV or EBV. Dually labelled MHC-I tetramers loaded with the same immunodominant peptide from either CMV-VTE, CMV-TPR, or EBV-RAK identify virus-specific CD8⁺ T cells from BM of HLA-typed donor #1 (percentages of specific cells is indicated in the gate); (E–G) Quantification of CMV- or EBV-specific CD8 T cells and the percentage of CD69⁺ cells therein, in human BM. Data are shown for *n* = 5 HLA-typed BM samples from five different donors; (E) Table describes detailed information on each specific T cell population detected; (F) The percentage of Tet⁺ cells detected within total CD8⁺ cells. For (F) and (G), results are shown as average ± SD. In panel (G), only those samples are indicated for which >100 CD69⁺ tetramer⁺ CD8⁺ T cells were acquired. Data was analyzed by one-way ANOVA followed by Tukey's multiple comparisons test (G) and two-way ANOVA, with matching, followed by Bonferroni's multiple comparison test (C). Significance is indicated by **p* < 0.05 and ***p* < 0.01.

compartment (T_{RM} cells). Next, we used our gene expression data to determine to what extent these BM T cell subsets are transcriptionally different from each other. We found the highest similarity between T_{RM} and T_{EM} cells (only 93 differentially expressed (DE) genes, FC > 1.5, RPKM > 8, *p* < 0.05), whereas T_{RM} cells were much more distinct from T_{CM} and T_{NV} cells (T_{RM} vs T_{CM} cells: 493 DE genes; T_{RM} vs T_{NV} cells: 927 DE genes) (Fig. 5A). From the

93 and 493 genes that are differentially expressed between T_{RM} versus T_{EM} and T_{RM} versus T_{CM}, respectively, we found 39 genes that are significantly different between resident and circulating memory CD8⁺ T cells in the BM (Fig. 5B and Supporting Information Table 1). From these 39 genes, nine belong to the aforementioned tissue residency signature that we recently described [13], such as *Klf2*, *S1pr1*, and *Zfp683* (Fig. 5C). Additionally, BM CD8⁺

Table 1. Tetrameric complexes used to detect virus-specific human CD8⁺ T cells by combinatorial coding

Tetramer specificity	HLA-restriction	Virus	Protein	Sequence	Amino acid positions
A1-CMV-VTE	HLA-A*0101	HCMV	pp50	VTEHDTLLY	245–253
A2-CMV-NLV	HLA-A*0201	HCMV	pp65	NLVPMVATV	495–504
B7-CMV-TPR	HLA-B*0702	HCMV	pp65	TPRVTGGGAM	417–426
A2-EBV-GLC	HLA-A*0201	EBV	BMLF-1	GLCTLVAML	259–267
B7-EBV-RPP	HLA-B*0702	EBV	EBNA-3A	RPPIFIRRL	247–255
B8-EBV-RAK	HLA-B*0802	EBV	BZLF-1	RAKFKQLL	190–197

T_{RM} cells express higher levels of *Itga1* (encoding CD49a) and *Cd101*, both also described in CD8⁺ T_{RM} cells from murine skin and human lung [9, 12], as well as other immune-related genes, such as *Tnfrsf10* (encoding TRAIL) and *Icosl* (Fig. 5C).

Gene ontology analysis on the DE genes between resident and circulating T cells (T_{RM} vs T_{EM} = 93 DE genes + T_{RM} vs T_{CM} = 493 DE genes, Total = 586 DE genes, RPKM > 8, FC > 1.5) yielded 104 Gene Ontology (GO) terms, which clustered into nine groups (Fig. 5D). According to their GO-term content (Supporting Information Table 2), BM CD8⁺ T_{RM} cells differed from their circulatory counterparts in categories related to T cell activation and differentiation, cytotoxicity, protein synthesis, leukocyte migration, and response to IFN- γ . Interestingly, the first cluster, with 23 GO-terms, is associated with the “Regulation of cytokine production and proliferation.” Because the most significant GO-term within this cluster is “Positive regulation of IFN- γ production” (Supporting Information Table 2), we determined the expression levels of IFN- γ in the different memory populations. We detected high levels of IFN- γ mRNA in T_{EM} and T_{RM} cells, both in the RNAseq dataset (Fig. 5E) and by RT-qPCR (Fig. 5F). To study the regulation of IFN- γ production, we analyzed IFN- γ protein expression by flow cytometry in LCMV-specific memory CD8⁺ T cells from BM without or with GP₃₃₋₄₁ peptide stimulation (Fig. 5G). Importantly, the expression of CD69 and CD62L did not change during the stimulation due to the addition of Brefeldin A, which allows reliable identification of the different T cell subsets following short antigenic stimulation (Fig. 5G and Supporting Information Fig. 3A). Interestingly, we found that BM CD8⁺ T_{RM} cells from LCMV-immune mice already produced IFN- γ without antigen stimulation, which was not observed in T_{CM} or T_{EM} cells (Fig. 5H). Upon the addition of cognate antigen, IFN- γ production rapidly increased in both T_{RM} and T_{EM}, but not T_{CM} cells (Fig. 5I). The percentage of IFN- γ -producing T cells upon activation was slightly lower for T_{RM} compared to T_{EM} cells (Fig. 5I), even though the frequency of D^b GP₃₃₋₄₁-specific cells was equal between these two groups (Supporting Information Fig. 3B). D^b NP₃₉₆₋₄₀₄-specific cells were more abundant within the T_{EM} than in the T_{RM} compartment and this was also seen for IFN- γ -producing T cells upon activation with the cognate peptide (Supporting Information Fig. 3C and D). In both cases, the amount of IFN- γ per cell was lower in T_{RM} than in T_{EM} (Supporting Information Fig. 3E and F). We also observed that all IFN- γ ⁺ T cells co-expressed CCL3 (Fig. 5J), a pro-inflammatory chemokine that can attract many different leukocytes through CCR1, CCR4, or CCR5, and

which is expressed in CD8⁺ T_{RM} cells (Supporting Information Table 2 and ref. [11]). Like their circulating counterparts, IFN- γ -producing CD8⁺ T_{RM} cells in the BM are highly polyfunctional, as they can coproduce significant amounts of IL-2 and/or TNF- α (Fig. 5K and L).

Gene expression analysis also indicated a distinct “Cytotoxicity” cluster for BM T_{RM} cells (Fig. 5D and Supporting Information Fig. 4A). As one of the genes in this cluster is Granzyme B (*Gzmb*), we analyzed protein levels by flow cytometry in LCMV-specific T cells; but despite higher mRNA levels, Granzyme B protein was hardly expressed in T_{RM} and T_{EM} cells, in particular when compared to LCMV-specific T_{EM} cells in spleen and peripheral blood (Supporting Information Fig. 4B and C). Yet, upon stimulation with LCMV peptide, BM CD8⁺ T_{RM} cells degranulated as indicated by expression of CD107a, demonstrating their cytotoxic ability (Supporting Information Fig. 4D and E). The percentage of CD107a⁺ T_{RM} cells was similar as T_{EM} cells in the BM, whereas the T_{RM} fraction had even higher expression of CD107a (Supporting Information Fig. 4F). These data indicate that although BM T_{RM} cells may not be loaded with cytotoxic granules in the steady state and capable of immediate cytotoxicity, they do have high transcript levels for genes involved in cytotoxicity and are able to degranulate upon activation, at least in a comparable fashion as BM T_{EM} cells.

Overall, these results indicate that BM CD8⁺ T_{RM} cells share important functional features with circulating CD8⁺ T_{EM} cells, such as rapid responsiveness to cognate antigen with polyfunctional cytokine production and cytotoxic potential, but they also have a gene expression pattern that is clearly distinctive from their circulating counterparts.

BM T_{RM} cells reside in the parenchyma in close contact with the circulation

We next investigated how CD8⁺ T_{RM} cells in BM related to CD8⁺ T_{RM} cells in other tissues. Therefore, we compared their transcriptional profile with our previously published dataset on CD8⁺ T_{RM} cells in liver, skin, and small intestines [13]. To compare both datasets, the gene expression in each subset was related to naïve splenic CD8⁺ T cells, as this population was a common denominator in both experimental designs. This analysis revealed that 136 of the 458 DE genes in BM CD8⁺ T_{RM} cells (FC > 2, RPKM > 8, $p < 0.05$) are shared between all organs, whereas 82 are unique to the BM (Fig. 6A). Comparison of these 82 genes to the genes

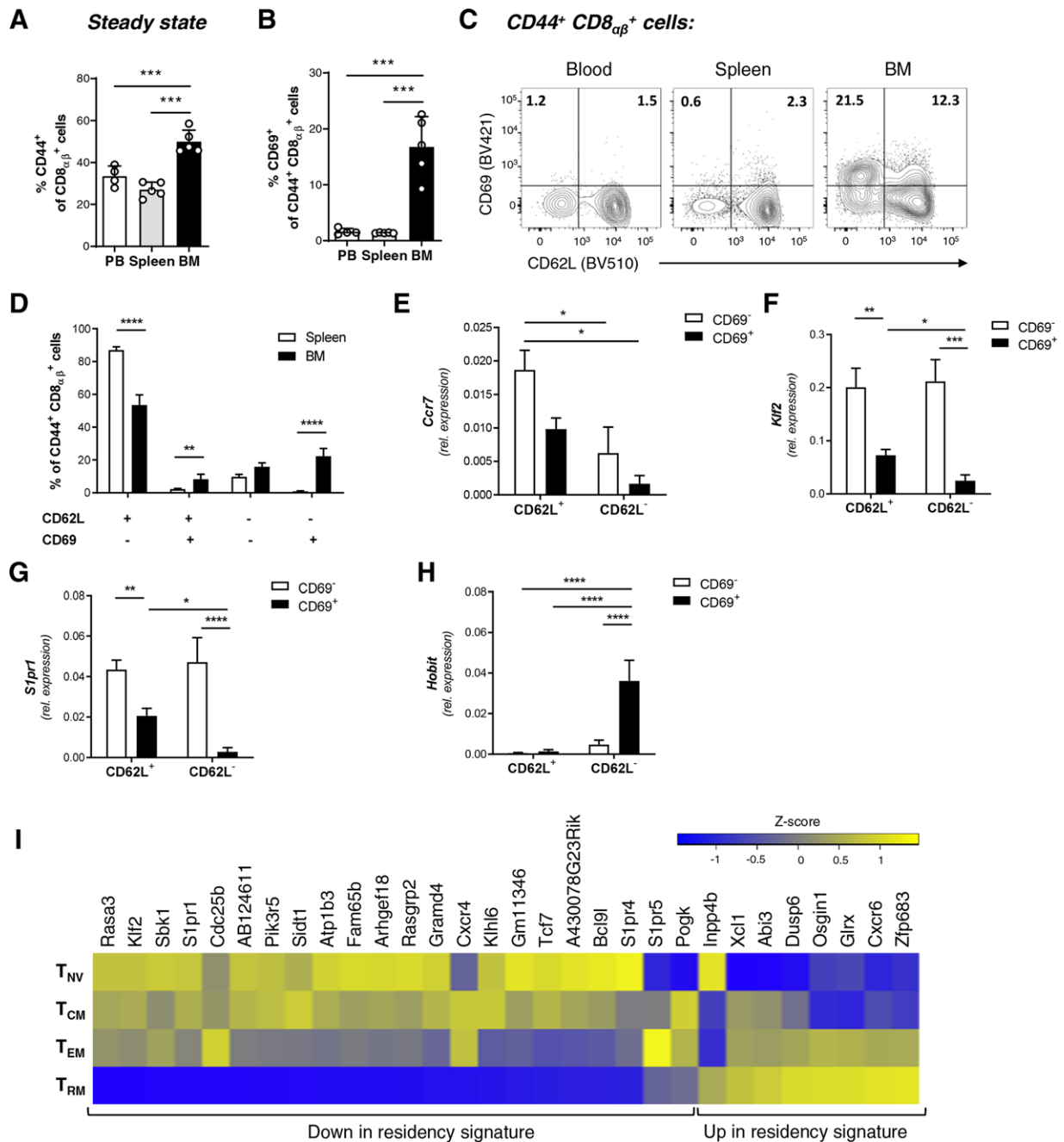


Figure 4. Murine steady-state BM lodges CD8⁺ T cell memory-like cells with a resident phenotype. (A–D) Analysis of the CD8⁺ T cell memory-like compartment in adult mice under SPF breeding. Data are shown for 1 experiment with $n = 5$ mice; (A) Frequency of memory CD44⁺ cells within CD8_{αβ}⁺ TCRβ⁺ T cells in peripheral blood (PB), spleen, and BM; (B) Frequency of CD69⁺ cells of all CD44⁺ CD8_{αβ}⁺ TCRβ⁺ T cells; (C) Representative FACS plots showing expression of CD62L and CD69 on memory CD8 T cells (defined as CD44⁺ CD8_{αβ}⁺ TCRβ⁺ cells) in the different organs; (D) Frequency of memory CD8⁺ T cell subsets in spleen and BM, as gated for in panel C; (E–H) Relative mRNA expression of (E) *Ccr7*, (F) *Klf2*, (G) *S1pr1*, and (H) *Hobit* relative to the housekeeping gene *Cyclophilin A* in sort-purified memory CD8⁺ T cell subsets from BM, as defined in (C) and (D). Data is shown for four independent sorting experiments, each with pooled BM from $n = 4$ mice; (I) Heatmap of RNA sequencing data for the 30 genes that compose the universal transcriptional signature of lymphocyte tissue residency [13] in CD8⁺ T_{NV} (CD44⁺ CD8_{αβ}⁺ TCRβ⁺), T_{CM} (CD44⁺ CD62L⁺ CD69⁻), T_{EM} (CD44⁺ CD62L⁻ CD69⁻), and T_{RM} (CD44⁺ CD62L⁻ CD69⁺) cells that were sort-purified from BM of naive mice. Data are shown from three independent sorting experiments, each with pooled BM from $n = 6$ mice. Relative expression levels (Z-scores) of genes are shown, color coded according to legend. Data are shown as mean ± SD (A and B) or mean ± SEM (E–H). Statistical analysis was performed with one-way ANOVA followed by Tukey's multiple comparisons test (A and B) and two-way ANOVA followed by Bonferroni's multiple comparison test (D–H). Significance is indicated by * $p < 0.05$; ** $p < 0.01$; *** $p < 0.001$; and **** $p < 0.0001$.

Table 2. Gene enrichment of tissue residency signature in BM T_{RM}-like cells

#	Gene symbol	FDR-corrected p-value		Average RPKM			
		T _{RM} versus T _{EM}	T _{RM} versus T _{CM}	T _{NV}	T _{CM}	T _{EM}	T _{RM}
1	Rasa3	ns	3.3×10^{-03}	115.0	100.3	91.8	44.1
2	Klf2	9.0×10^{-26}	7.0×10^{-41}	173.3	123.6	77.9	9.4
3	Sbk1	9.8×10^{-04}	4.7×10^{-03}	32.7	23.1	26.0	10.4
4	S1pr1	1.2×10^{-09}	3.9×10^{-18}	160.1	114.4	64.1	9.7
5	Cdc25b	9.2×10^{-08}	1.5×10^{-03}	23.2	24.0	33.7	10.3
6	AB124611	ns	5.0×10^{-03}	58.8	54.4	39.8	20.2
7	Pik3r5	ns	ns	79.0	78.7	65.7	48.3
8	Sidt1	4.1×10^{-04}	4.2×10^{-19}	87.0	110.2	54.5	20.9
9	Atp1b3	2.4×10^{-02}	8.0×10^{-09}	247.2	192.0	132.5	64.0
10	Fam65b	ns	ns	66.2	51.5	44.3	27.1
11	Arhgef18	ns	9.5×10^{-03}	87.8	70.0	56.3	34.5
12	Rasgrp2	2.7×10^{-03}	1.6×10^{-08}	66.0	41.2	30.8	13.1
13	Gramd4	1.0×10^{-04}	2.2×10^{-26}	112.5	84.5	37.9	14.8
14	Cxcr4	ns	ns	64.4	75.9	75.0	56.1
15	Klhl6	ns	6.4×10^{-06}	90.0	93.4	47.3	29.7
16	Gm11346	ns	1.3×10^{-05}	38.4	20.8	11.9	6.2
17	Tcf7	ns	3.3×10^{-03}	562.4	459.9	265.9	195.8
18	A430078G23Rik	ns	1.5×10^{-02}	73.7	51.2	31.7	22.6
19	Bcl9l	ns	3.7×10^{-03}	80.7	50.6	34.3	23.8
20	S1pr4	ns	ns	100.8	61.6	58.1	41.7
21	S1pr5	7.9×10^{-03}	ns	0.1	2.1	19.7	1.1
22	Pogk	ns	1.9×10^{-04}	2.7	18.1	14.0	7.2
23	Inpp4b	ns	ns	41.6	21.5	19.9	33.0
24	Xcl1	ns	ns	0.7	56.8	69.6	158.2
25	Abi3	ns	ns	1.0	1.9	2.0	2.4
26	Dusp6	ns	4.5×10^{-11}	4.3	18.1	38.6	79.5
27	Osgin1	ns	ns	0.3	0.2	1.2	1.7
28	Glrx	ns	2.9×10^{-02}	9.2	7.6	16.4	20.9
29	Cxcr6	ns	3.0×10^{-20}	39.6	61.8	185.7	360.2
30	Zfp683	2.8×10^{-03}	2.8×10^{-34}	2.7	3.7	45.8	164.9

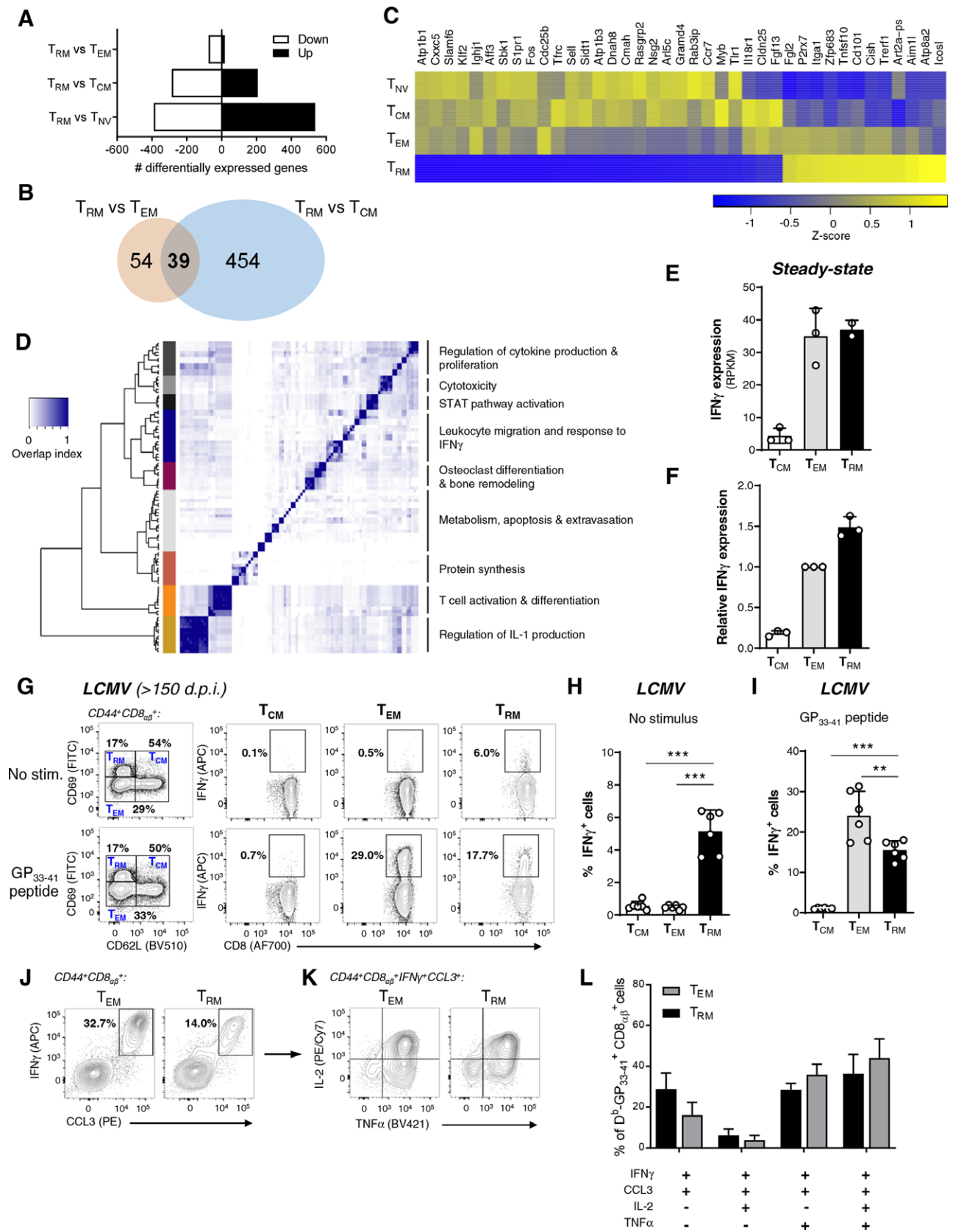
differentially expressed between resident and recirculating memory BM T cells, revealed that the expression of 28 genes is unique to BM T_{RM} cells and is not expressed in the circulating memory CD8⁺ T cell subsets in the BM. They include genes such as *Sulf2* (regulates binding of chemokines/cytokines to the ECM), *Mmp9* (involved in tissue remodeling), *Chst2* (involved in biosynthesis of chondroitin sulfate proteoglycans), *Vav3* (involved in adhesion via β -integrins), three transcriptional activators/repressors (*Zbtb42*, *Maf*, and *Trerf1*), and *Icosl*.

A pairwise correlation of the 136 genes that were shared between CD8⁺ T_{RM} cells in all four tissues revealed that BM T_{RM} are more similar to T_{RM} cells in the liver than in the small intestine (SI) or skin (Fig. 6B). A striking difference between these three organs is their localization of CD8⁺ T_{RM} cells, as skin and SI CD8⁺ T_{RM} cells are located within the epithelium and detect antigen coming from their local environment, while liver T_{RM} cells are found inside the liver sinusoids and can respond to blood-derived antigens [4, 28, 38]. To assess the localization of BM T_{RM} cells and their exposure to the blood stream, we examined their ability to rapidly bind an intravenously injected anti-CD8 α antibody [39]. As expected, both blood and liver CD8 β ⁺

CD44⁺ cells showed the highest degree of staining after intravascular injection of anti-CD8 α antibody, while the spleen had two populations, one protected from and one accessible to the anti-CD8 α antibody (Fig. 6C), which relates to their location in the white and red pulp, respectively [39]. Interestingly, BM CD8 β ⁺ CD44⁺ T cells showed some degree of intravascular staining (Fig. 6D), which was comparable between all three memory subsets (Fig. 6E). These results suggest a parenchymal, rather than sinusoidal localization, for all CD8⁺ memory T cell subsets in the BM, which was confirmed by immunofluorescent staining of CD8⁺ T cells on BM sections (Fig. 6F). Moreover, staining for CD69 further corroborated the parenchymal distribution of both CD69⁺ and CD69⁻ CD8⁺ T cells (Fig. 6G and Supporting Information Fig. 5).

Maintenance of BM T_{RM} cells depends on IL-15, Blimp-1, and Hobit

The BM is rich in IL-15-producing stromal cells [40] that provide a niche for long-term maintenance of memory T cells [14, 41].



As the dependence of T_{RM} cells on IL-15 varies per tissue [22], we investigated whether BM $CD8^+ T_{RM}$ cells depend on IL-15 for their long-term maintenance. Therefore, we transferred in vitro-activated gBT-I $CD8^+$ T cells into WT or IL-15-deficient animals (IL-15^{-/-}), and we analyzed the BM for total gBT-I and $CD69^+$ gBT-I T cells after 30 days (Fig. 7A). We detected gBT-I T cells in both WT and IL-15^{-/-} recipients (Fig. 7B), although we observed a significant decrease of $CD69^+$ gBT-I cells in the IL-15^{-/-} recipients (Fig. 7C). This finding indicates that $CD8^+ T_{RM}$ cells in the BM are dependent on IL-15 signaling.

It has been shown that $CD8^+ T_{RM}$ cells in a variety of tissue sites are dependent on the expression of the transcription factors Blimp-1 and Hobit [13]. Therefore, we next analyzed how the genetic deletion of these transcription factors affected the development of $CD8^+ T_{RM}$ cells in the BM. Following infection with influenza virus, we found that the percentage of total virus-specific $CD8^+$ T cells was not different in WT, *Blimp1*^{-/-}, *Hobit*^{-/-}, or *Blimp1*^{-/-}*xHobit*^{-/-} mice >60 days post-intranasal infection (Fig. 7D). However, the percentage of $CD69^+$ cells within the *D^b-NP₃₆₆₋₃₇₄*⁺ cells was significantly reduced in the *Blimp1*^{-/-}*xHobit*^{-/-} mice (Fig. 7E). Altogether, these results indicate that BM parenchyma hosts $CD8^+ T_{RM}$ cells that depend on Blimp-1 and Hobit for their generation and/or maintenance.

The pool of BM $CD8^+ T_{RM}$ cells is expandable

Human CMV infection is associated with increased levels of IL-15 mRNA in the BM, together with an accumulation of $CD8^+ CD45RA^+ CD27^-$ memory T cells, that are highly responsive to IL-15 [42]. We questioned whether the inflationary accumulation of memory T cells seen during murine CMV infection (MCMV) [43] would also lead to inflation of the BM T_{RM} pool. To address this, we analyzed the frequency of $CD8^+$ T cells in the BM that were specific for acute (M45, M57) and latent inflationary

(M38, m139) epitopes in MCMV >60 days after infection. $CD69^+ CD62L^- CD44^+ CD8_{\alpha\beta}^+$ T cells were detected for both acute and inflationary epitopes at this time point (Fig. 8A and B). However, whereas BM T_{EM} cells were significantly enriched for inflationary epitopes, this was not the case for BM T_{RM} cells, which showed a similar size for all tested epitopes (Fig. 8C). This would indicate that MCMV-induced memory inflation favors $CD8^+ T_{EM}$ rather than T_{RM} cells, but it could also be that there is a restriction in the pool size or occupancy of the niches that maintain the $CD8^+ T_{RM}$ cells in the BM. To investigate the latter, we transferred OVA-specific OT-I cells to naive WT mice and challenged them either once or thrice with OVA in different ways (Fig. 8D). More than 30 days after the last challenge, we observed a significant increase in the percentage of OT-I cells in mice that were challenged thrice, compared to mice that were challenged only once (Fig. 8E). This strong expansion was observed for both the T_{RM} and T_{EM} OT-I cells (Fig. 8F), indicating that the BM T_{RM} pool can expand upon antigen re-encounter. Yet, it was possible that after three immunizations the $CD8^+ T_{RM}$ niche was still not fully occupied. We reasoned that full occupancy of the niche might be achieved by consecutive infections with more complex pathogens. To address this, we challenged mice with *Listeria*-OVA on day 0, after which the mice were infected on day 30 with LCMV Armstrong or not, followed by analysis on day 60 for $CD8^+$ memory T cells in the BM specific for either pathogen (Fig. 8G and Supporting Information Fig. 6A and B). Importantly, these experiments revealed that the generation of new $CD8^+ T_{RM}$ cells against LCMV did not affect the size of the preexisting pool of $CD8^+ T_{RM}$ cells against *Listeria*-OVA (Fig. 8H). In fact, the total population of $CD8^+ T_{RM}$ cells in the BM expanded 2.6-fold after the second infection (Fig. 8I). Comparable results were obtained when we performed the inverse experiment, i.e., first LCMV, followed by *Listeria*-OVA (Supporting Information Fig. 6C–F). We, therefore, conclude that the pool of $CD8^+ T_{RM}$ cells in the BM is readily expandable and can increase in both size and diversity when the host is exposed to new antigenic challenges.

Figure 5. Specific features of BM $CD8^+ T_{RM}$ cells. (A–D) Analysis of RNA sequencing data obtained for $CD8^+ T_{NV}$ (*CD44*⁻ *CD62L*⁺), T_{CM} (*CD44*⁺ *CD62L*⁺), T_{EM} (*CD44*⁺ *CD62L*⁻ *CD69*⁻), and T_{RM} (*CD44*⁺ *CD62L*⁻ *CD69*⁺) cells that were sort-purified from BM of naive mice. Data are shown from three independent sorting experiments, each with pooled BM from *n* = 6 mice; (A) Number of differentially expressed (DE) genes (downregulated in white, upregulated in black) between T_{RM} versus T_{EM} , T_{RM} versus T_{CM} , and T_{RM} versus T_{NV} . DE expressed genes were specifically up- or downregulated in BM T_{RM} in comparison to their circulating counterparts, as determined by RNA sequencing (fold change [FC] > 1.5; and reads per kilobase per million mapped reads (RPKM) > 8); (B) Venn diagram showing the overlap between genes DE by T_{RM} and T_{EM} , T_{RM} , and T_{CM} cells; (C) Heatmap displays relative amounts of transcripts of the 39 DE genes that were shared in the comparison shown in (B). Relative expression levels (Z-scores) of genes are shown, color coded according to legend; (D) Correlation of gene ontology (GO)-terms enriched in the sum of DE expressed genes between T_{RM} versus T_{EM} and T_{RM} versus T_{CM} (547 DE genes, FC > 1.5; RPKM = 8). GO-terms were filtered to contain between 20 and 100 genes. Enrichment analysis revealed enrichment of the DE genes in 104 GO-terms, which clustered into nine groups by comparison of their overlap index. Results are shown as a heatmap of the overlap indices, with the clustering and a color representation of each group on the left and a representative group name on the right; (E and F) Transcript levels of IFN- γ in T_{CM} , T_{EM} , and T_{RM} sorted from steady-state mice, analyzed via RNAseq (E, obtained as in A–D) or RT-qPCR (F, data are from four different sorting experiments, each with pooled BM from *n* = 4 mice); (G–I) Production of IFN- γ by T_{CM} , T_{EM} , or T_{RM} $CD8^+$ T cells from LCMV-infected mice. BM cells were incubated for 5 h with Brefeldin A in the absence (no stim.) or presence of GP₃₃₋₄₁ peptide and IFN- γ production was evaluated by ICS in the different memory populations. Data are shown for one representative experiment with *n* = 4 mice, out of two independent experiments; (G) Representative plots and quantification of the production of IFN- γ in the absence (H) or presence of LCMV peptide (I); (J and K) Polyfunctionality of T_{EM} and T_{RM} cells was analyzed as in panels (G–I). Data are from one representative experiment with *n* = 5 mice, out of two independent experiments; (L) Co-production of IFN- γ and CCL3 by T_{EM} or T_{RM} $CD8^+$ T cells from LCMV-infected mice. Representative plots (K) and quantification (L) of T_{EM} and T_{RM} capable of simultaneously producing two, three, or four out of four cytokines (IFN- γ , CCL3, IL-2, and TNF- α). Results in (H), (I), and (L) show mean \pm SD. Statistical analysis was performed by one-way ANOVA followed by Tukey's multiple comparisons test. Significance is indicated by ***p* < 0.01 and ****p* < 0.001.

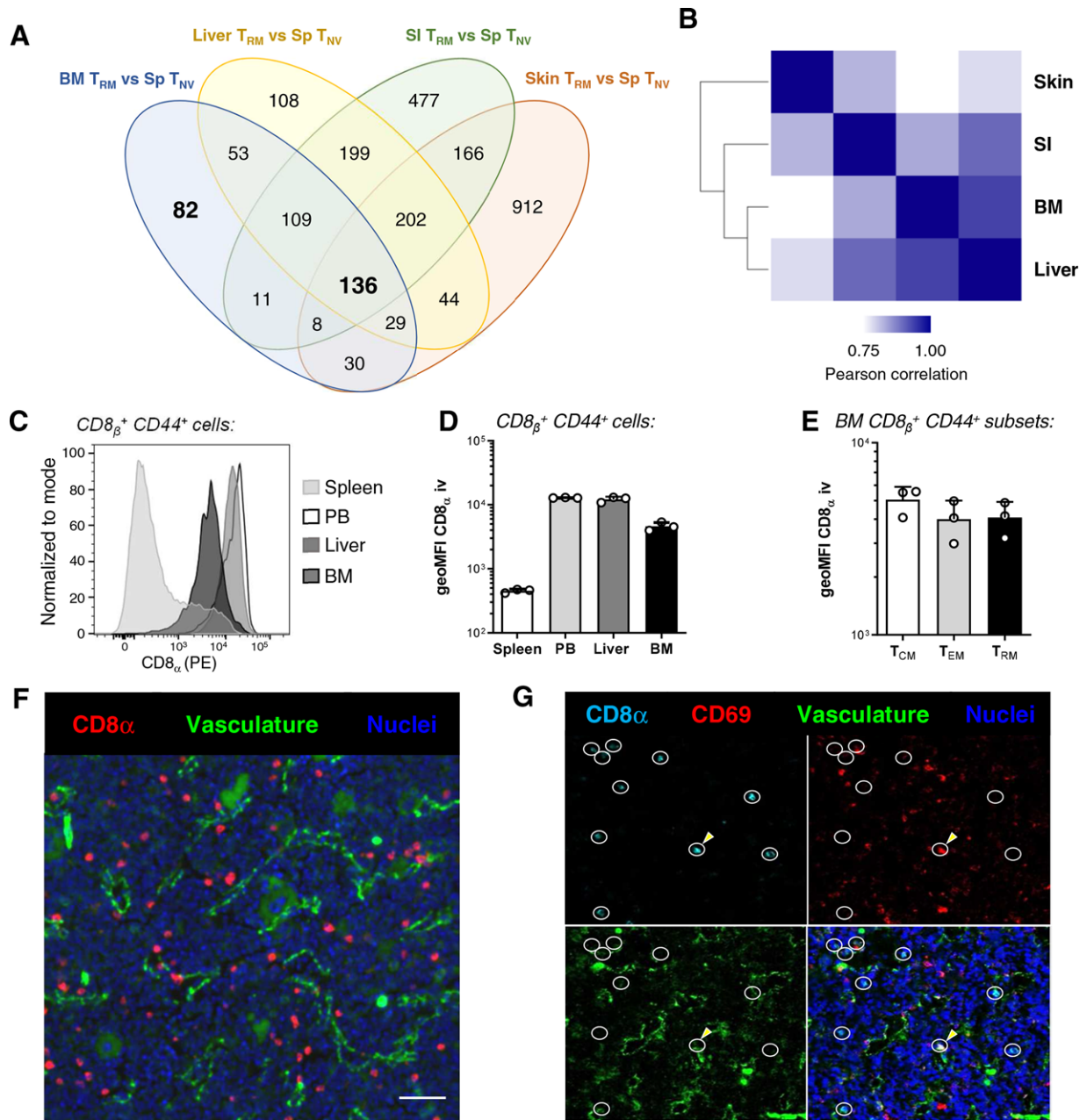


Figure 6. BM $CD8^{+} T_{RM}$ cells reside in the parenchyma in close contact with the circulation. (A and B) Comparison of DE genes between T_{RM} from different organs. RNA sequencing data for BM T_{RM} was acquired as in Fig. 4I, while data for liver, SI, and skin T_{RM} were obtained from ref. [13]; (A) Venn diagram showing the overlap between DE genes by T_{RM} from BM, Liver, SI, and skin, compared to splenic T_{NV} (Sp) ($FC > 1.5$; RPKM = 8); (B) Correlation plot depicting the similarity between T_{RM} in different organs. The correlation is pairwise, and was calculated using \log_2 RPKM values of the 136 DE genes that were significant in all four contrasts; (C–E) Intravascular staining to probe the localization of T_{RM} within the BM. Mice were i.v. injected with 3 μ g of an antibody against CD8 $_{\alpha}$. Organs were obtained 2 min after injection and processed immediately. Data are shown for one representative experiment with $n = 3$ mice, out of two independent experiments; (C) A representative histogram comparing the staining with the anti-CD8 $_{\alpha}$ antibody in $CD8_{\beta}^{+} CD44^{+}$ cells from spleen, peripheral blood (PB), liver, and BM; geoMFI of CD8 $_{\alpha}$ staining in (D) $CD8_{\beta}^{+} CD44^{+}$ cells from the different organs or (E) $CD8_{\beta}^{+}$ memory subsets within the BM; (F and G) Immunofluorescence analysis of (F) $CD8_{\alpha}^{+}$ cells or (G) $CD69^{+} CD8_{\alpha}^{+}$ cells within steady-state BM. Scale bar = 50 μ m. Vasculature was visualized with antibodies against CD31 and CD144 and nuclei with Helix NP green staining. One representative region from a tile scan of 4×7 images is shown. The full tile scan is shown in Supporting Information Fig. 2; $40\times$ magnification. Each $CD8_{\alpha}^{+}$ cell is encircled in white to identify these cells across the different stainings. $CD69^{+} CD8_{\alpha}^{+}$ cells are marked with an arrow.

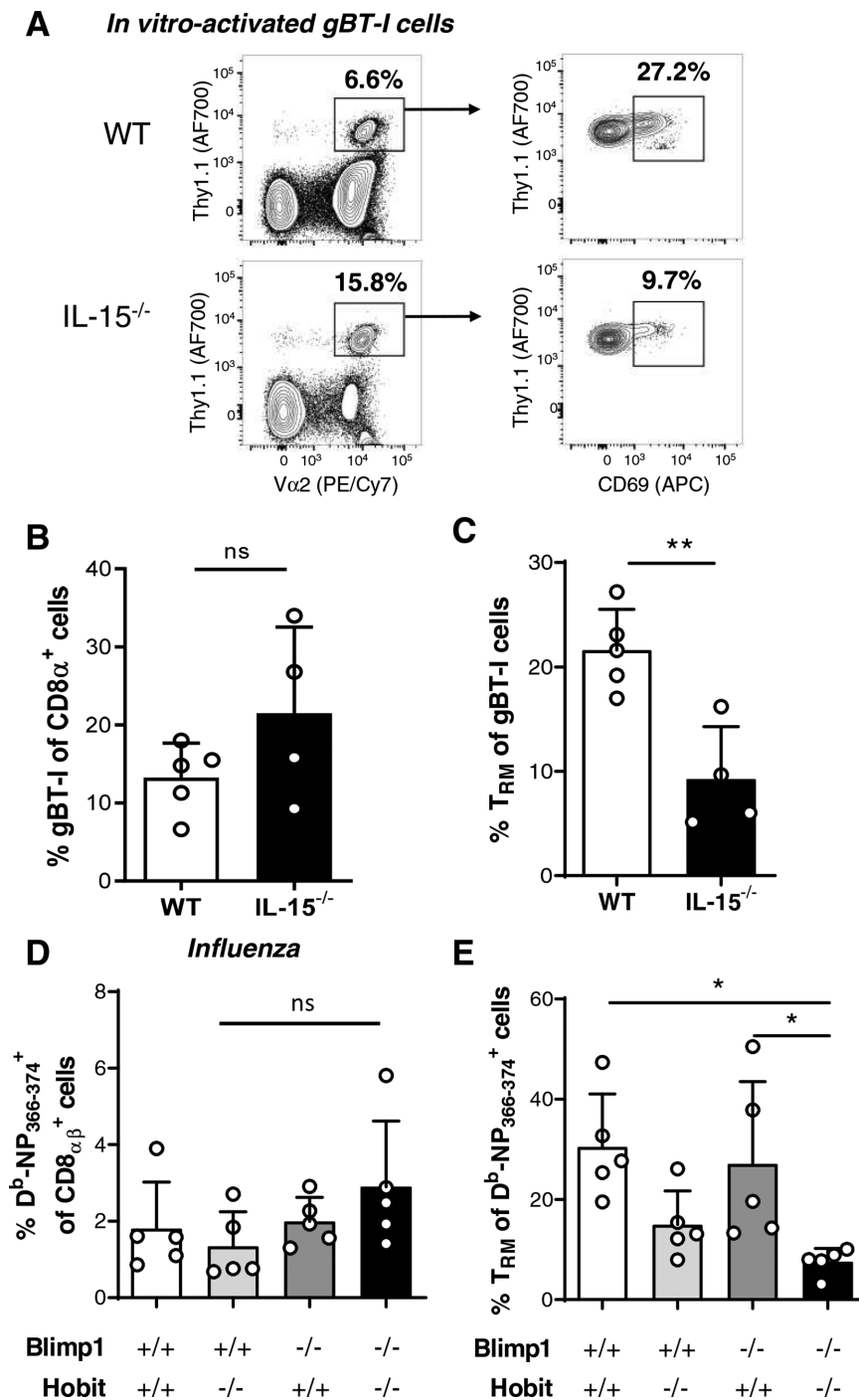


Figure 7. Maintenance of BM CD8⁺ T_{RM} cells depends on IL-15 and Hobit. (A–C) In vitro-activated gBT-I cells were transferred into WT or IL-15^{-/-} mice and, after 30 days, the presence of total gBT-I and CD69⁺ gBT-I was analyzed in the BM. Results are shown as (A) representative plots, (B) quantification of the % of gBT-I within total CD8 α ⁺ cells and (C) quantification of TRM (CD69⁺) cells within gBT-I cells in the BM, from one experiment with $n = 5$ WT and 4 IL-15^{-/-} mice. Results show mean \pm SD; experiment was performed twice. (D and E) WT (Blimp^{+/+} Hobit^{+/+}) or mice deficient for Hobit (Blimp^{+/+} Hobit^{-/-}), Blimp1 (Blimp^{-/-} Hobit^{+/+}), or both (Blimp^{-/-} Hobit^{-/-}) were infected i.n. with Influenza A/HKx31. BM was harvested and analyzed 63 dpi. Results are shown from one representative experiment with $n = 5$ mice, out of three independent experiments, as (D) percentage of D^b-NP₃₆₆₋₃₇₄⁺ cells within total CD8 $\alpha\beta$ ⁺ T cells and (E) percentage of T_{RM} (CD69⁺ CD62L⁻) cells within D^b-NP₃₆₆₋₃₇₄⁺ CD8 $\alpha\beta$ ⁺ T cells. Data were analyzed by two-tailed t-test (B and C) or one-way ANOVA followed by Tukey's multiple comparisons test (D and E). Significance is indicated by * $p < 0.05$ and ** $p < 0.01$.

Discussion

Here, we show that the BM harbors an expandable pool of bona fide resident memory CD8⁺ T cells that develop in response to peripheral antigen recognition. BM CD8⁺ T_{RM} cells share transcriptional similarities with other tissue-resident lymphoid cells found in a variety of organs, while also expressing a unique set of genes related to tissue remodeling and adhesion, which is likely

induced by the BM environment. We demonstrate that BM CD8⁺ T_{RM} cells are polyfunctional cytokine producers and depend on IL-15, and the transcription factors Blimp-1 and Hobit for their maintenance.

Both human [14, 16] and murine BM [17–19] contain a large number of memory T cells. In this work, we demonstrate that the BM, in contrast to the spleen, contains a unique subset of CD62L⁻ CD69⁺ memory T cells, both in the steady-state and after

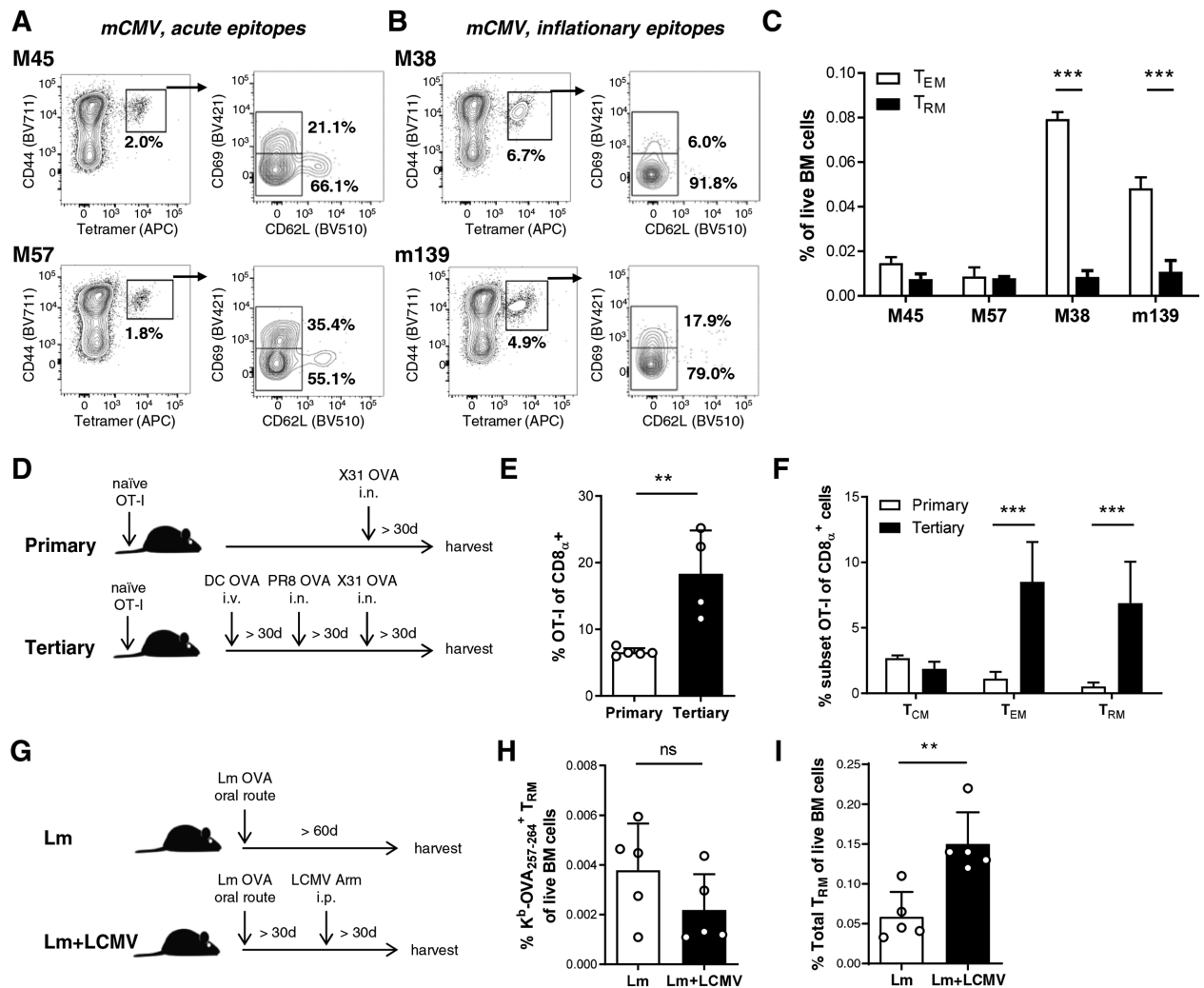


Figure 8. The pool of BM $CD8^+ T_{\text{RM}}$ cells is expandable. (A–C) Distribution of $CD8_{\text{eff}}^+$ memory populations specific for mCMV acute and inflationary epitopes analyzed 65 days p.i.; Representative plots are shown for (A) acute epitopes M45 and M57 and (B) inflationary epitopes M38 and m139. Tetramer stainings are shown in the left panels and the gating for T_{RM} ($CD62L^+ CD69^+$) and T_{EM} ($CD62L^- CD69^+$) is shown in the right panels; (C) Percentage of T_{EM} and T_{RM} within live BM cells for each mCMV-specific population. Data is shown for one representative experiment with $n = 4$ mice, out of two independent experiments; (D–F) Distribution of OT-I memory populations analyzed more than 30 days after the last immunization in mice that received one or three homologous boosts to generate OVA-specific memory. Data are shown for one experiment with $n = 5$ mice that received one challenge and 4 mice that received three challenges; (D) Schematic depiction of the experimental setup; (E) Percentage of OT-I cells within total $CD8_{\text{eff}}^+$ cells in the BM; (F) Percentage of T_{CM} , T_{EM} , and T_{RM} within OT-I cells in the BM after one or three homologous challenges; (G–I) Distribution of OVA-specific $CD8_{\text{eff}}^+$ memory populations analyzed more than 60 days after the first challenge in mice that received only Lm-OVA or Lm-OVA followed by LCMV Armstrong infection, more than 30 days after the first challenge. Data are shown for one experiment with $n = 5$ mice/group. Results from the reverse experiment are shown in Supporting Information Fig. 3; (G) Schematic depiction of the experimental setup; (H) Percentage of $K^b\text{-OVA}_{257-264}^+$ T_{RM} cells of live BM cells; (I) Percentage of total T_{RM} within live BM cells. Data were analyzed by two-tailed t-test (E, H, and I) and two-way ANOVA, followed by Bonferroni's multiple comparison test (C and F). Significance is indicated by ** $p < 0.01$ and *** $p < 0.001$.

a variety of infectious challenges. Our results suggest that the enrichment in memory $CD8^+$ T cells in BM compared to spleen can be largely attributed to the presence of resident cells. These results fit with previous observations that show that, compared to matched PB, the human BM is enriched for $CD8^+$ T cells with a T_{EM} ($CD45RA^- CCR7^-$) phenotype [14, 36], and that $CD69^+$ cells are present among the T_{EM} and T_{EMRA} subsets ($CD45RA^+ CCR7^-$) in this organ. Additionally, human BM is enriched for $CD8^+$ T cells expressing CXCR6 and CCR5, as well as $CD8^+$ T cells specific for an epitope from EBV lytic protein BZLF-1, but not for

$CD8^+$ T cells specific for epitopes from EBV latent protein EBNA3A or CMV pp65 [36]. We observed that CXCR6 and CCR5 expression is significantly higher in $CD69^+$ than in $CD69^- CD8^+$ BM T cells and the percentage of $CD69^+$ is higher in $CD8^+$ T cells specific for the same EBV lytic epitope than in CMV-specific $CD8^+$ T cells. Altogether, these results suggest that both human and murine BM are enriched for $CD8^+$ T_{RM} cells and these comprise a true reservoir of systemic memory, in the sense that they are maintained in the organ at disequilibrium with the circulatory pool. The recirculating behavior of the $CD69^-$ memory $CD8^+$ subsets present in the BM,

i.e., T_{EM} and T_{CM} cells, remains to be addressed. It is possible that a part of these populations also resides in the BM, but our data—from the parabiosis experiments and RNAseq analysis—support the notion that most of them are in equilibrium with the circulatory pool.

Certain tissues, such as brain and lung, require local antigen recognition for $CD8^+ T_{RM}$ cell development [44, 45], whereas other organs intrinsically support T_{RM} cell lodgment and survival in the absence of antigen [21, 34, 46]. Previous work on $CD4^+$ T cells in human BM showed a preferential recruitment and/or maintenance of long-term T-cell memory for systemic pathogens (measles, rubella, and mumps) versus that for skin or mucosal pathogens (*Candida albicans* and Vaccinia virus) [16], suggesting that local antigen presentation might be required for BM T_{RM} cells. Yet, we could demonstrate that both systemic (LCMV, Listeria) and peripheral (Influenza, HSV) infections led to the generation of antigen-specific $CD8^+ T_{RM}$ in the BM, as did transfer of in vitro activated TCR-transgenic $CD8^+$ T cells, demonstrating that local antigen recognition is not necessary for the establishment of $CD8^+ T_{RM}$ cells in the BM. The difference with what has been suggested for human $CD4^+$ BM T cells could be explained by several factors, such as differences between human versus mouse, or differential requirements for the development of $CD4^+$ versus $CD8^+ T_{RM}$ cells. The requirements for human $CD8^+ T_{RM}$ generation are to date largely unexplored.

In several organs, $CD8^+ T_{RM}$ cells are not in contact with the circulation, but rather localized in close association with the epithelium, since this is where they are most likely to re-encounter their cognate antigen [39]. The liver is an exception to this rule, as liver T_{RM} cells are lining the sinusoids, which enables them to re-encounter their antigen arriving via the bloodstream. Interestingly, we found for the BM that $CD8^+ T_{RM}$ cells reside inside the parenchyma, but they are still in close connection to the vasculature, given their rapid intermediate level of staining with an intravenously injected anti- $CD8\alpha$ antibody. This is also true for the other $CD8^+$ T cell subsets in the BM, and thus a likely consequence of the high permeability of the BM sinusoids [47], rather than a specific feature of the $CD8^+ T_{RM}$ cells. We recently confirmed the perivascular localization of memory $CD8^+$ T cells in the BM, which is most likely driven by their CXCR4 expression and the CXCL12-expressing stromal cells around the BM sinusoids [48]. Both $CD4^+$ and $CD8^+$ T cell populations are evenly distributed throughout the BM parenchyma [17], and we also did not observe a different localization for $CD69^+$ compared to $CD69^- CD8^+$ cells. Nevertheless, it is conceivable that the BM does have specialized niches for different $CD8^+$ T cell subsets, as we found that $CD8^+ T_{RM}$ cells in BM depend on IL-15, whereas $CD69^-$ memory $CD8^+$ T cells do not. We have previously shown that IL-15 can induce expression of Hobit, which induces a subset of genes that prevents egress and increases tissue interactions [13]. IL-15-expressing VCAM-1⁺ stromal cells are scattered throughout the entire BM [40], making it possible that local IL-15 signaling contributes to the generation of $CD8^+ T_{RM}$ cells through the induction of Hobit. Yet, immunofluorescent imaging suggests that IL-15-expressing stromal cells are more abundant than $CD8^+ T_{RM}$ cells in the BM; moreover, these

stromal cells are likely to harbor also other memory $CD8^+$ T cell subsets in the BM, as most memory T cells are in direct contact with IL-7⁺ VCAM-1⁺ stromal cells [17], and these largely overlap with IL-15-expressing cells [40]. We, therefore, postulate that although IL-15 triggering is required for the generation of $CD8^+ T_{RM}$ cells, it is most likely not sufficient, and their development may depend also on other intrinsic and/or extrinsic signals.

Another important issue regarding the generation of T_{RM} cells is the expandability of the pool, because of its implications in vaccine design and the development of protective tissue memory. Just as the total pool of circulating memory T cells can expand upon repetitive challenges [49], the pool of $CD8^+ T_{RM}$ can dramatically grow in size in barrier tissues, like the skin [34, 50], where the size of the pool directly correlates with protection [50]. Because the BM is a hematopoietically active compartment with a fixed cellularity and little space to expand due to the encompassing bone, we addressed whether the pool of BM $CD8^+ T_{RM}$ cells could expand or if there would competition for niche signals. Remarkably, the number of BM $CD8^+ T_{RM}$ cells specific for a single antigenic peptide could indeed expand upon multiple immunizations. In agreement with this, when mice were sequentially challenged with two different pathogens, BM $CD8^+ T_{RM}$ cells against the first pathogen were not deleted to make space for newly formed T_{RM} against the second challenge. Instead, the total pool of BM $CD8^+ T_{RM}$ cells grew in size to accommodate the new specificities. These observations reinforce the concept of the BM as an expandable reservoir for long-term memory. It remains to be shown whether this reservoir can contribute to the systemic pool upon re-challenge, especially after long periods between generation and re-encounter with the cognate antigen.

The implications of this resident, long-term memory storage in the BM are intriguing. It could be that $CD8^+ T_{RM}$ cells have a protective function in the BM, comparable to their role in liver, brain, and barrier tissues [28, 46, 51]. Yet, in contrast to liver T_{RM} [52], BM T_{RM} cells did not contain preformed Granzyme B in their cytotoxic granules and are thus less likely to exert immediate cytotoxicity upon re-challenge. Human BM $CD8^+$ T cells with an effector memory phenotype, of which more than 70% expressed CD69, were also shown to contain much lower levels of Perforin and Granzyme B compared to paired samples of peripheral blood [25]. Furthermore, BM T_{RM} cells specific for Influenza or HSV are also not likely to be protective to the tissue, as these pathogens do not infect the BM; however, it is conceivable that these T_{RM} cells do get activated when neutrophils bring antigens from the periphery to the BM, thereby driving local T cell activation [33]. This may lead to proliferation of BM T_{RM} cells, comparable to skin and female reproductive tract [9, 53], and the formation of effector T cells that leave the BM and provide protection in the infected organ. $CD8^+ T_{EM}$ and T_{CM} cells in the BM are known to be major contributors to the organ's memory reservoir function [15, 25], and these subsets outnumber the T_{RM} cells in the BM. It is therefore interesting to speculate that T_{RM} cells in the BM may also fulfill a different function. Memory $CD8^+$ T cells support engraftment of hematopoietic stem and progenitor cells upon transplantation [54] and enhance the maintenance of

hematopoietic stem cells (HSCs) [23]. This could be important during viral infections, when HSCs are lost due to increased differentiation and impaired self-renewal (reviewed by Pascutti et al. [55]). Influx of memory CD8⁺ T cells in the BM following viral infection may serve to prevent or restore the HSC pool, and it is conceivable that CD8⁺ T_{RM} cells also play a role in this process. This is corroborated by our observation that BM CD8⁺ T_{RM} cells spontaneously produce IFN- γ , given that the production of IFN- γ during the steady state is beneficial for the pool of HSCs [56, 57]. This implies a role for BM T_{RM} cells during homeostasis, although they also rapidly upregulate IFN- γ upon activation, by which they may contribute to skewing hematopoiesis towards the type of immune cell that is beneficial for eradicating the invading pathogen (reviewed in ref. [58]). It could thus well be that CD8⁺ T_{RM} cells in the BM not only have an immune protective role, but also support the local hematopoietic process, though this requires further investigation.

In conclusion, the BM harbors a subset of memory CD8⁺ T cells that are not part of the recirculating pool, but that have taken up residency in the parenchyma of the BM. Given their broad range of specificities and ability to respond to and expand upon antigenic re-challenge, we believe that these cells constitute an attractive target for protective vaccination strategies.

Materials and methods

Mice

C57BL/6J mice were purchased from Janvier Labs. For steady state analysis, mice were aged in the NKI animal facility and studied between the ages of 16 and 30 weeks. *Zfp683*^{-/-} (Hobit KO [59]), *Prdm1*^{fllox/fllox} \times Lck Cre (Blimp1 KO [60]) and IL-15^{-/-} (IL-15 KO [61]) mice were maintained on a C57BL/6J background. Blimp1 KO mice were crossed onto Hobit KO mice to generate Blimp1 \times Hobit double KO (Blimp1 \times Hobit DKO) mice. gBT-I mice are CD8⁺ TCR transgenic mice that recognize the H-2K^b-restricted HSV-1 gB epitope of amino acids 498–505 (gB₄₉₈₋₅₀₅, SSIEFARL) [46]. Mice were maintained under SPF conditions and animal experiments were performed according to national and institutional guidelines.

Infections, immunizations, and cell transfers

Mice were infected with either LCMV (intraperitoneal route [i.p.], 2×10^5 PFU Armstrong), *Listeria*-OVA (intravenous route, 1×10^4 CFU or oral route, 2×10^9 CFU), Influenza A/HKx31 (x31, H3N2, intranasal route [i.n.], $10 \times 50\%$ tissue culture-infective dose), Influenza A/HKx31-OVA (x31-OVA, H3N2, i.n., 1×10^4 PFU), Influenza A/PR8/34-OVA (PR8, H1N1, i.p., 1.5×10^7 PFU), HSV type 1 KOS (epicutaneous application after scarification, 1×10^6 PFU), or MCMV-Smith (intraperitoneal route, 1×10^4 PFU). For the HSV-1 infections, naïve gBT-I cells (5×10^4 cells) were injected

intravenously (i.v.) prior to HSV infection. In vitro-generated gBT-I effector splenocytes were activated by peptide-pulsed splenocytes as described previously [9], of which 5×10^6 cells were injected i.v. in either WT and IL-15^{-/-} mice. Multiple immunizations were performed by administering OVA-peptide loaded BM-derived DCs, followed by infection with PR8-OVA and later Influenza x31-OVA. BM-derived DCs were generated by culture of BM cells for 7 days in the presence of 20 ng/mL GM-CSF and IL-4 to allow for DC differentiation. DC were then matured overnight in the presence of 150 ng/mL LPS and pulsed with OVA₂₅₇₋₂₆₄ peptide (SIINFEKL, 1 μ g/mL, 45 min) prior to transfer. Then 2.5×10^5 DC were transferred i.v. into recipients. Mice were sacrificed at the indicated time points after infection or cell transfer and organs were harvested for analysis.

Murine tissue collection and preparation

Single cell preparations of spleen were obtained by passing organs over a 70 μ m cell strainer (BD Biosciences) with MACS buffer (PBS + 1% FCS + 2 mM EDTA). Bones were harvested, cleaned, and crushed in MACS buffer using a mortar and pestle. BM cell suspensions were filtered through a 70 μ m cell strainer to remove bone debris. Erythrocytes were lysed with lysis buffer (155 mM NH₄Cl, 10 mM KHCO₃, 127 mM EDTA). For intravascular stainings, 3 μ g of PE-labeled anti-CD8 α (53-6.7) antibody was injected i.v. 2 min before sacrificing the mice. All organs were harvested and processed immediately.

Flow cytometry analysis of murine samples

Single cell suspensions were labeled with the indicated fluorescently conjugated antibodies at 4°C for 30 min in PBS containing 1% FCS. The antibodies used were purchased from eBioscience, BD Biosciences, or BioLegend: CD44 (IM7), CD62L (MEL-14), CD69 (H1.2F3), CD8 α (53-6.7), CD8 β (YTS156.7.7), and TCR β (H57-597). Virus-specific CD8⁺ T cells were examined with the following MHC class I tetramers: D^b-GP₃₃₋₄₁ (LCMV, KAVYN-FATC) and D^b-NP₃₉₆₋₄₀₄ (LCMV, FQPQNGQFI), K^b-OVA₂₅₇₋₂₆₄ (*Listeria*-OVA, SIINFEKL), D^b-NP₃₆₆₋₃₇₄ (LCMV, ASNENMETM), D^b-M45₉₈₅₋₉₉₃ (MCMV, HGIRNASFI), K^b-M57₈₁₆₋₈₂₄ (MCMV, SCLEFWQRV), K^b-M38₃₁₆₋₃₂₃ (MCMV, SSPPMFRV), and K^b-m139₄₁₉₋₄₂₆ (MCMV, TVYGFCLL). MHC class I peptide tetramers for K^b-OVA₂₅₇₋₂₆₄ and D^b-NP₃₆₆₋₃₇₄ were kind gifts from Dr. Derk Amsen (Sanquin, Amsterdam, The Netherlands). Tetramer labeling was performed at room temperature. Adoptively transferred gBT-I cells were identified by their expression of the TCR α -chain variable region 2 (V α 2 (B20.1)) and Thy1.1 (HIS51). For ICS, 1×10^6 splenocytes or 5×10^6 BM cells were cultured in the presence or absence of peptide (2 μ g/mL) and brefeldin A for 5 h at 37°C. Staining was carried out with the BD Cytofix/Cytoperm kit, using antibodies against CCL3 (DNT3CC), IFN- γ (XMG1.2), IL-2 (JES6-5H4), and TNF- α (MP6-XT22). Samples were collected by an LSR Fortessa (BD) and analyzed with FlowJo software

(Tree Star). For analysis, cells were fixed in 0.5% paraformaldehyde (PFA). Dead cells were excluded with LIVE/DEAD[®] Fixable Near-IR Dead Cell Stain Kit (Thermo Fisher Scientific), following manufacturer's instructions. Cells were acquired on an LSR Fortessa (BD Biosciences) flow cytometer and analyzed with FlowJo software (Tree Star, Inc.).

Parabiosis experiments

Parabiosis experiments were performed as described by Collins et al. [62]. In short, 5×10^4 gBT-I CD45.1⁺ cells were transferred i.v. into WT CD45.2⁺ mice and then the mice were infected with HSV. Alternatively, mice received in vitro activated gBT-I cells. In the memory phase (HSV = 40 days; in vitro-activated = 11 months), these mice were conjoined to non-infected CD45.2⁺ control mice. Each mouse was anesthetized with ketamine (100 mg/kg) and xylazine (15 mg/kg). Skin was shaved and disinfected with alcohol and betadine pads. Matching incisions were made from the olecranon to the knee joint of each mouse and subcutaneous fascia was bluntly dissected to create 0.5 cm of free skin. The olecranon and knee joints were attached by a 5-0 silk suture, and dorsal and ventral skins were attached by continuous staples or sutures. Betadine was used to disinfect the entire incision following surgery. Both mice of each pair were injected subcutaneously with PBS and buprenorphine (0.1 mg/kg) to treat pain. Three weeks after conjoining, the mice were sacrificed and the presence and phenotype of CD45.1⁺ gBT-I donor cells in spleens and BM were analyzed in all mice.

Human BM analysis

BM samples were obtained from allo-SCT donors after approval of the Leiden University Medical Center institutional review board and informed consent according to the Declaration of Helsinki. Informed consent form all participants involved in this study were written for samples obtained since 2003 and verbal for older samples when guidelines provided no written consent. Bone marrow mononuclear cells (BMMC) were isolated by Ficoll gradient centrifugation, and frozen in liquid nitrogen until further analysis. For T cell staining of approximately 1×10^6 BMMC a final concentration of 2 μ g/mL per pMHC tetramer was added and incubated for 15 min at 37°C. Next, antibody-mix was added and cells were incubated for 30 min at 4°C. Prior to flow cytometry, cells were washed twice. Dual-encoding pMHC tetramer analysis was performed as previously described [37] and description of the tetramer complexes used is shown in Table 1. The following antibodies from ThermoFisher, BD, or Biolegend were used: anti-CD8 (3B5), anti-CD3 (UCHT1), anti-CD69 (FN50), anti-CD103 (Ber-ACT8), anti-CXCR6 (K041E5), anti-CX₃CR1 (2A9-1), and anti-CCR5 (J418F1). Near-IR fixable dye (Invitrogen) was used to exclude dead cells from the analysis. All samples were measured in PBS 0.5% FCS with an LSR Fortessa (BD) and the analysis was performed using FlowJo Version 10 software.

Immunofluorescence staining

Bones were embedded in Tissue-Tek OCT compound (Sakura Finetek) and cooled with liquid nitrogen. Sections of 8 mm were made with a cryostat (Leica) using the CryoJane Tape-Transfer System (Leica). Sections were fixed in acetone, air-dried, and blocked with CAS-Block (Thermo Fisher Scientific) for 15 min, and subsequently stained with antibodies in PBS/1% BSA. Primary antibodies were stained O/N at 4°C, followed by secondary antibodies for 1–2 h at room temperature. The following antibodies were used: CD8 α -Alexa Fluor 647 (53-6.7, Biolegend), CD144/VE-cadherin biotin (BV13, Biolegend), CD31/PECAM-1 biotin (MEC 13.3, BD Pharmingen), CD69 (R&D systems), Donkey-Anti-Goat IgG Alexa Fluor 568 (Invitrogen), and Streptavidin eFluor 450 (eBioscience). Nuclei were stained using Helix NP green (eBioscience). Sections were viewed using a SP8 confocal (Leica). Images were further processed in LASX (Leica) and Fiji Imaging Software.

Quantitative PCR

RNA was extracted using TRIzol (Invitrogen) and complementary DNA was made with random hexamers and Superscript II reverse transcriptase (Roche). Quantitative real-time PCR was performed in duplicate with Express SYBR Green reagents (Invitrogen) on the StepOnePlus RT-PCR system (Applied Biosystems), and data were normalized using Cyclophilin A as reference gene. Primer sequences are available upon request.

RNA sequencing

For sorting, CD8⁺ T cells from spleen and BM were pooled and enriched with CD8 α microbeads (Miltenyi Biotec) and MACS LS columns (Miltenyi Biotec) (6 mice/sort, three sorts in total). The following subsets of CD8 $\alpha\beta$ ⁺ T cells were sorted to purity on an FACSaria II or III (BD Biosciences): T_{RM} (CD44⁺CD62L⁻CD69⁺), T_{EM} (CD44⁺CD62L⁻CD69⁻), T_{CM} (CD44⁺CD62L⁺), and T_{NV} (CD44⁻CD62L⁺). RNA was isolated with the NucleoSpin RNA XS kit (Macherey-Nagel). A DNase treatment step was performed during the isolation. RNA quality check, polyA RNA selection and sequencing were performed at GenomeScan BV (Leiden, The Netherlands). RNA quality and quantity was determined by a Bioanalyzer Picochip (Agilent). Per sample, 25 ng RNA was used for library preparation and single-end, 75 nt fragments were analyzed by Illumina NextSeq 500. At least 20×10^6 reads were analyzed and mapped to the mouse genome (UCSC, mm10) with TopHat (v2.1.0). Reads that aligned to (exonic parts of) genes annotated by Ensembl (release 78) were quantified using featureCounts (v1.4.3-p1). Differential gene expression analysis was done with edgeR (version 3.14.0) in R (v3.3.1). Genes that had less than 1 CPM (counts per million mapped reads) in less than three samples were removed. A negative binomial generalized log-linear model was fit to the data. Pair-wise comparisons (contrasts) were made between the different cell populations, and glmTreat

was used to find genes that had at least 1.5- (comparisons between BM subsets) or 2- (comparisons between T_{RM} and T_{NV} in different organs) fold change difference. Genes with FDR-adjusted p -values < 0.05 were considered significantly differentially expressed, if they also had at least eight RPKMs (reads per kilobase of transcript per million mapped reads) in one or both of the two cell types that were compared in the contrasts. Data are available from GEO under accession number GSE96839.

GO-term enrichment analysis was done using the Wallenius method including gene length bias in *goseq* (v1.24.0), followed by *gogadget* (v2.0) [63] in R (v3.3.2). Enrichment was done using the genes that were differentially expressed in either the BM T_{RM} versus BM T_{CM} cells comparison, and/or the BM T_{RM} versus BM T_{EM} cells comparison, combined, restricting on only biological processes (BP). In *gogadget*, enriched GO-terms (FDR-adjusted p -value < 0.05) were first filtered so that only terms containing more than 20 but less than 100 genes were left, and were subsequently clustered using the overlap index, with Ward.D method and Manhattan distance.

To compare T_{RM} cells from BM to T_{RM} cells from other organs (liver, small intestine (SI), and skin), RNA-Seq data from ref. [13] were downloaded (GEO accession: GSE70813), and were also mapped to the mouse genome similar as described above. In *edgeR* the same filtering criteria were used, and batch effect (both experiments) was taken into account in the model. Differentially expressed genes between BM T_{RM} versus liver T_{RM} , BM T_{RM} versus SI T_{RM} , and BM T_{RM} versus skin T_{RM} were again defined as genes that differed at least twofold change, and had at least eight RPKMs in one or both groups.

To find a BM T_{RM} specific signature, gene expression of T_{RM} cells per organ (BM, liver, SI, and skin) were compared with that of naïve T cells from the spleen. Here, differentially expressed genes were defined more stringent, analogous to ref. [13], FDR-adjusted p -values < 0.05 , at least twofold change difference, and eight RPKMs in one or both groups. The differentially expressed genes uniquely found in the BM T_{RM} versus spleen naïve T cells were further used for GO-term enrichment analysis. In *gogadget*, all BP enriched GO-terms were clustered using the overlap index, with Ward.D method and Euclidean distance.

Statistical analysis

Statistical analyses were performed with Prism (GraphPad Software, Inc.) using t -test, one-way or two-way ANOVA, depending on the experimental design. Significance is indicated by $*p < 0.05$, $**p < 0.01$, $***p < 0.001$, and $****p < 0.0001$.

Acknowledgements: The authors appreciate the animal facility for excellent care of the mice and the Central Facility of Sanquin for their indispensable help with flow cytometry, sorting, and microscopy. The authors thank the Adaptive Immunity group

and the T cell biology group at Sanquin Research for helpful discussions and Prof. Dr. Rene van Lier for critical reading of the manuscript. S.G. and M.F.P. were financially supported by a Fellowship obtained by M.A.N. from the Landsteiner Foundation for Blood Transfusion Research. K.P.v.G. was supported by Vidi grant 917.13.338 from NWO and a fellowship of the Landsteiner Foundation of Blood Transfusion Research.

Author contributions: M.F.P., S.G., N.C., M.W., M.H.M.H., P.H., R.A., L.K.M., K.P.J.M.v.G., and M.A.N. designed the research. M.F.P., S.G., N.C., G.B., R.S., F.B., A.O., E.S., E.P., J.E.P., S.H., and P.H. performed the research. M.F.P., S.G., N.C., G.B., B.N., A.O., J.E.P., P.H., and M.A.N. analyzed the data. M.H.M.H. and R.A. provided essential biological material. M.F.P., S.G., M.W., and M.A.N. wrote the manuscript.

Conflict of interest: The authors declare no financial or commercial conflict of interest.

References

- Sallusto, F., Lenig, D., Förster, R., Lipp, M. and Lanzavecchia, A., Two subsets of memory T lymphocytes with distinct homing potentials and effector functions. *Nature*. 1999. 401: 708–712.
- Matloubian, M., Lo, C. G., Cinamon, G., Lesneski, M. J., Xu, Y., Brinkmann, V., Allende, M. L. et al., Lymphocyte egress from thymus and peripheral lymphoid organs is dependent on S1P receptor 1. *Nature*. 2004. 427: 355.
- Mueller, S. N. and Mackay, L. K., Tissue-resident memory T cells: local specialists in immune defence. *Nat. Rev. Immunol.* 2015. 16: 1–11.
- Schenkel, J. M. and Masopust, D., Tissue-resident memory T cells. *Immunity*. 2014. 41: 886–897.
- Mackay, L. K., Braun, A., Macleod, B. L., Collins, N., Tebartz, C., Bedoui, S., Carbone, F. R. et al., Cutting Edge: CD69 Interference with Sphingosine-1-Phosphate Receptor Function Regulates Peripheral T Cell Retention. *J. Immunol.* 2015. 194: 2059–2063.
- Shiow, L. R., Rosen, D. B., Brdičková, N., Xu, Y., An, J., Lanier, L. L., Cyster, J. G. and Matloubian, M., CD69 acts downstream of interferon- α/β to inhibit S1P1 and lymphocyte egress from lymphoid organs. *Nature*. 2006. 440: 540–544.
- Steinert, E. M., Schenkel, J. M., Fraser, K. A., Beura, L. K., Manlove, L. S., Igyártó, B. Z., Southern, P. J. et al., Quantifying memory CD8 T cells reveals regionalization of immunosurveillance. *Cell*. 2015. 161: 737–749.
- Beura, L. K., Mitchell, J. S., Thompson, E. A., Schenkel, J. M., Mohammed, J., Wijeyesinghe, S., Fonseca, R. et al., Intravital mucosal imaging of CD8⁺ resident memory T cells shows tissue-autonomous recall responses that amplify secondary memory article. *Nat. Immunol.* 2018a. 19: 173–182.
- Park, S. L., Zaid, A., Hor, J. L., Christo, S. N., Prier, J. E., Davies, B., Alexandre, Y. O. et al., Local proliferation maintains a stable pool of tissue-resident memory T cells after antiviral recall responses. *Nat. Immunol.* 2018. 19: 183–191.
- Ariotti, S., Hogenbirk, M. A., Dijkgraaf, F. E., Visser, L. L., Hoekstra, M. E., Song, J.-Y., Jacobs, H. et al. Skin-resident memory CD8⁺ T cells trigger a state of tissue-wide pathogen alert. *Science*. 2014. 346: 101–105.
- Schenkel, J. M., Fraser, K. A., Vezys, V. and Masopust, D., Sensing and alarm function of resident memory CD8(+) T cells. *Nat Immunol.* 2013. 14: 509–513.

- 12 Kumar, B. V., Ma, W., Miron, M., Friedman, A. L., Shen, Y., Farber, D. L., Granot, T. et al. Human tissue-resident memory T cells are defined by core transcriptional and functional signatures in lymphoid and mucosal sites. *Cell Rep.* 2017. 20: 2921–2934.
- 13 Mackay, L. K., Minnich, M., Kragten, N. A. M. M., Liao, Y., Nota, B., Seillet, C., Zaid, A. et al. Hobit and Blimp1 instruct a universal transcriptional program of tissue residency in lymphocytes. *Science* (80-). 2016. 352: 459–463.
- 14 Herndler-Brandstetter, D., Landgraf, K., Jenewein, B., Tzankov, A., Brunauer, R., Brunner, S., Parson, W. et al. Human bone marrow hosts polyfunctional memory CD4+ and CD8+ T cells with close contact to IL-15-producing cells. *J. Immunol.* 2011. 186: 6965–6971.
- 15 Mazo, I. B., Honczarenko, M., Leung, H., Cavanagh, L. L., Bonasio, R., Weninger, W., Engelke, K. et al. Bone marrow is a major reservoir and site of recruitment for central memory CD8+ T cells. *Immunity.* 2005. 22: 259–270.
- 16 Okhrimenko, A., Grün, J. R., Westendorf, K., Fang, Z., Reinke, S., von Roth, P., Wassilew, G. et al. Human memory T cells from the bone marrow are resting and maintain long-lasting systemic memory. *Proc. Natl. Acad. Sci. U. S. A.* 2014. 111: 9229–9234.
- 17 Sercan Alp, Ö., Durlanik, S., Schulz, D., McGrath, M., Grün, J. R., Bardua, M., Ikuta, K. et al. Memory CD8+ T cells colocalize with IL-7+ stromal cells in bone marrow and rest in terms of proliferation and transcription. *Eur. J. Immunol.* 2015. 45: 975–987.
- 18 Tokoyoda, K., Zehentmeier, S., Hegazy, A. N., Albrecht, I., Grün, J. R., Löhning, M. and Radbruch, A., Professional Memory CD4+ T Lymphocytes Preferentially Reside and Rest in the Bone Marrow. *Immunity.* 2009. 30: 721–730.
- 19 Geerman, S., Hickson, S., Brassier, G., Pascutti, M. F. and Nolte, M. A., Quantitative and qualitative analysis of bone marrow CD8+ T cells from different bones uncovers a major contribution of the bone marrow in the vertebrae. *Front. Immunol.* 2016. 6: 660.
- 20 Wang, Y., Godec, J., Ben-Aissa, K., Cui, K., Zhao, K., Pucsek, A. B., Lee, Y. K. et al. The transcription factors T-bet and runx are required for the ontogeny of pathogenic interferon- γ -producing T helper 17 cells. *Immunity* 2014. 40: 355–366.
- 21 Casey, K. A., Fraser, K. A., Schenkel, J. M., Moran, A., Abt, M. C., Beura, L. K., Lucas, P. J. et al. Antigen-independent differentiation and maintenance of effector-like resident memory T cells in tissues. *J. Immunol.* 2012. 188: 4866–4875.
- 22 Schenkel, J. M., Fraser, K. A., Casey, K. A., Beura, L. K., Pauken, K. E., Vezy, V. and Masopust, D., IL-15-independent maintenance of tissue-resident and boosted effector memory CD8 T cells. *J. Immunol.* 2016. 196: 3920–3926.
- 23 Geerman, S., Brassier, G., Bhushal, S., Salerno, F., Kragten, N. A., Hoogenboezem, M., de Haan, G. et al. Memory CD8+ T cells support the maintenance of hematopoietic stem cells in the bone marrow. *Haematologica* 2018. 103. <https://doi.org/10.3324/haematol.2017.169516>.
- 24 Pritz, T., Landgraf-Rauf, K., Herndler-Brandstetter, D., Rauf, R., Lair, J., Gassner, R., Weinberger, B. et al. Bone marrow T cells from the femur are similar to iliac crest derived cells in old age and represent a useful tool for studying the aged immune system. *Immun. Ageing.* 2013. 10: 17.
- 25 Zhang, X., Dong, H., Lin, W., Voss, S., Hinkley, L., Westergren, M., Tian, G. et al. Human bone marrow: a reservoir for “enhanced effector memory” CD8+ T cells with potent recall function. *J. Immunol.* 2006. 177: 6730–6737.
- 26 Di Rosa, F. and Gebhardt, T., Bone Marrow T Cells and the Integrated Functions of Recirculating and Tissue-Resident Memory T Cells. *Front. Immunol.* 2016. 7: 1–13.
- 27 Siracusa, F., Alp, Ö. S., Maschmeyer, P., McGrath, M., Mashreghi, M. F., Hojyo, S., Chang, H. D. et al. Maintenance of CD8+ memory T lymphocytes in the spleen but not in the bone marrow is dependent on proliferation. *Eur. J. Immunol.* 2017. 47: 1900–1905.
- 28 Fernandez-Ruiz, D., Ng, W. Y., Holz, L. E., Ma, J. Z., Zaid, A., Wong, Y. C., Lau, L. S. et al., Liver-resident memory CD8+ T cells form a front-line defense against malaria liver-stage infection. *Immunity* 2016. 0: 2–12.
- 29 Zaid, A., Hor, J. L., Christo, S. N., Groom, J. R., Heath, W. R., Mackay, L. K. and Mueller, S. N., Chemokine Receptor-Dependent Control of Skin Tissue-Resident Memory T Cell Formation. *J. Immunol.* 2017. 199: 2451 LP-2459.
- 30 Bergsbaken, T., Bevan, M. J. and Fink, P. J., Local inflammatory cues regulate differentiation and persistence of CD8+ tissue-resident memory T cells. *Cell Rep.* 2017. 19: 114–124.
- 31 Khan, T. N., Mooster, J. L., Kilgore, A. M., Osborn, J. F. and Nolz, J. C., Local antigen in nonlymphoid tissue promotes resident memory CD8+ T cell formation during viral infection. *J. Exp. Med.* 2016. 213: 951–966.
- 32 Hermesh, T., Moltedo, B., Moran, T. M. and López, C. B., Antiviral instruction of bone marrow leukocytes during respiratory viral infections. *Cell Host Microbe.* 2010. 7: 343–353.
- 33 Duffy, D., Perrin, H., Abadie, V., Benhabiles, N., Boissonnas, A., Liard, C., Descours, B. et al. Neutrophils transport antigen from the dermis to the bone marrow, initiating a source of memory CD8+ T cells. *Immunity* 2012. 37: 917–929.
- 34 Jiang, X., Clark, R. A., Liu, L., Wagers, A. J., Fuhlbrigge, R. C. and Kupper, T. S., Skin infection generates non-migratory memory CD8+ T RM cells providing global skin immunity. *Nature* 2012. 483: 227–231.
- 35 Klonowski, K. D., Williams, K. J., Marzo, A. L., Blair, D. A., Lingenheld, E. G. and Lefrançois, L., Dynamics of blood-borne CD8 memory T cell migration in vivo. *Immunity* 2004. 20: 551–562.
- 36 Palendira, U., Chinn, R., Raza, W., Piper, K., Pratt, G., Machado, L., Bell, A. et al. Selective accumulation of virus-specific CD8+ T cells with unique homing phenotype within the human bone marrow. *Blood* 2008. 112: 3293–3302.
- 37 Hadrup, S. R., Bakker, A. H., Shu, C. J., Andersen, R. S., van Veluw, J., Hombrink, P., Castermans, E. et al. Parallel detection of antigen-specific T cell responses by combinatorial encoding of MHC multimers. *Nat. Methods* 2009. 6: 520–526.
- 38 Pallett, L. J., Davies, J., Colbeck, E. J., Robertson, F., Hansi, N., Easom, N. J. W., Burton, A. R. et al., IL-2 high tissue-resident T cells in the human liver: sentinels for hepatotropic infection. *J. Exp. Med.* 2017. 214: 1567.
- 39 Anderson, K. G., Mayer-Barber, K., Sung, H., Beura, L., James, B. R., Taylor, J. J., Qunaj, L. et al. Intravascular staining for discrimination of vascular and tissue leukocytes. *Nat. Protoc.* 2014. 9: 209–222.
- 40 Cui, G., Hara, T., Simmons, S., Wagatsuma, K., Abe, A., Miyachi, H., Kitano, S. et al. Characterization of the IL-15 niche in primary and secondary lymphoid organs in vivo. *Proc. Natl. Acad. Sci. USA* 2014. 111: 1915–1920.
- 41 Becker, T. C., Coley, S. M., Wherry, E. J. and Ahmed, R., Bone marrow is a preferred site for homeostatic proliferation of memory CD8 T cells. *J. Immunol.* 2005. 174: 1269–1273.
- 42 Pangrazzi, L., Naismith, E., Meryk, A., Keller, M., Jenewein, B., Trieb, K. and Grubeck-Loebenstien, B., Increased IL-15 production and accumulation of highly differentiated CD8+ effector/memory T cells in the bone marrow of persons with cytomegalovirus. *Front. Immunol.* 2017. 8: 1–9.
- 43 Snyder, C. M., Cho, K. S., Bonnett, E. L., van Dommelen, S., Shellam, G. R. and Hill, A. B., Memory inflation during chronic viral infection is maintained by continuous production of short-lived, functional T cells. *Immunity* 2008. 29: 650–659.

- 44 McMaster, S. R., Wein, A. N., Dunbar, P. R., Hayward, S. L., Cartwright, E. K., Denning, T. L. and Kohlmeier, J. E., Pulmonary antigen encounter regulates the establishment of tissue-resident CD8 memory T cells in the lung airways and parenchyma. *Mucosal Immunol.* 2018. 11: 1071–1078.
- 45 Wakim, L. M., Woodward-Davis, A., Bevan, M. J. and Overhauser, N., Memory T cells persisting within the brain after local infection show functional adaptations to their tissue of residence. *Proc. Natl. Acad. Sci. USA* 2009. 107: 1231–1236.
- 46 Mackay, L. K., Stock, A. T., Ma, J. Z., Jones, C. M., Kent, S. J., Mueller, S. N., Heath, W. R. et al. Long-lived epithelial immunity by tissue-resident memory T (TRM) cells in the absence of persisting local antigen presentation. *Proc. Natl. Acad. Sci. USA* 2012. 109: 7037–7042.
- 47 Itkin, T., Gur-Cohen, S., Spencer, J. A., Schajnovitz, A., Ramasamy, S. K., Kusumbe, A. P., Ledergor, G. et al. Distinct bone marrow blood vessels differentially regulate haematopoiesis. *Nature* 2016. 532: 323–328.
- 48 Goedhart, M., Gessel, S., van der Voort, R., Slot, E., Lucas, B., Gielen, E., Hoogenboezem, M. et al. CXCR4, but not CXCR3, drives CD8 T-cell entry into and migration through the murine bone marrow. *Eur. J. Immunol.* 2019. 49: 576–589.
- 49 Vezyz, V., Yates, A., Casey, K. A., Lanier, G., Ahmed, R., Antia, R., Masopust, D. et al. Memory CD8 T-cell compartment grows in size with immunological experience. *Nature* 2009. 457: 196–199.
- 50 Davies, B., Prier, J. E., Jones, C. M., Gebhardt, T., Carbone, F. R. and Mackay, L. K., Cutting edge: tissue-resident memory T cells generated by multiple immunizations or localized deposition provide enhanced immunity. *J. Immunol.* 2017. 198: 2233–2237.
- 51 Schenkel, J. M., Masopust, D., Fraser, K. A., Beura, L. K., Pauken, K. E., Vezyz, V. and Masopust, D., Resident memory CD8 T cells trigger protective innate and adaptive immune responses. *Science* 2014. 346: 98–101.
- 52 Kragten, N. A. M., Behr, F. M., Vieira Braga, F. A., Remmerswaal, E. B. M., Wesselink, T. H., Oja, A. E., Hombrink, P. et al. Blimp-1 induces and Hobit maintains the cytotoxic mediator granzyme B in CD8 T cells. *Eur. J. Immunol.* 2018. 48: 1644–1662.
- 53 Beura, L. K., Wijeyesinghe, S., Thompson, E. A., Macchietto, M. G., Rosato, P. C., Pierson, M. J., Schenkel, J. M. et al. T cells in nonlymphoid tissues give rise to lymph-node-resident memory T cells. *Immunity* 2018b. 48: 327–338.e5.
- 54 Geerman, S. and Nolte, M. A., Impact of T cells on hematopoietic stem and progenitor cell function: good guys or bad guys? *World J. Stem Cells.* 2017. 9: 37.
- 55 Pascutti, M. F., Erkelens, M. N. and Nolte, M. A., Impact of viral infections on hematopoiesis: from beneficial to detrimental effects on bone marrow output. *Front. Immunol.* 2016. 7: 364.
- 56 Baldridge, M. T., King, K. Y., Boles, N. C., Weksberg, D. C. and Goodell, M. A., Quiescent haematopoietic stem cells are activated by IFN- γ in response to chronic infection. *Nature* 2010. 465: 793.
- 57 de Bruin, A. M., Demirel, O., Hooibrink, B., Brandts, C. H. and Nolte, M. A., Interferon-gamma impairs proliferation of hematopoietic stem cells in mice. *Blood* 2013. 121: 3578–3585.
- 58 de Bruin, A. M., Voermans, C. and Nolte, M. A., Impact of interferon-gamma on hematopoiesis. *Blood* 2014. 124: 2479–2486.
- 59 Van Gisbergen, K. P. J. M., Kragten, N. A. M., Hertoghs, K. M. L., Wensveen, F. M., Jonjic, S., Hamann, J., Nolte, M. A. et al. Mouse Hobit is a homolog of the transcriptional repressor Blimp-1 that regulates NKT cell effector differentiation. *Nat. Immunol.* 2012. 13: 864–871.
- 60 Kallies, A., Xin, A., Belz, G. T. and Nutt, S. L., Blimp-1 transcription factor is required for the differentiation of effector CD8⁺ T cells and memory responses. *Immunity* 2009. 31: 283–295.
- 61 Kennedy, M. K., Glaccum, M., Brown, S. N., Butz, E. A., Viney, J. L., Embers, M., Matsuki, N. et al., Reversible defects in natural killer and memory CD8 T cell lineages in interleukin 15-deficient mice. *J. Exp. Med.* 2000. 191: 771–780.
- 62 Collins, N., Jiang, X., Zaid, A., Macleod, B. L., Li, J., Park, C. O., Haque, A. et al., Skin CD4⁺ memory T cells exhibit combined cluster-mediated retention and equilibration with the circulation. *Nat. Commun.* 2016. 7: 1–13.
- 63 Nota, B., Gogadget: an R package for interpretation and visualization of GO enrichment results. *Mol. Inform.* 2017. 36. <https://doi.org/10.1002/minf.201600132>.

Abbreviations: CMV: cytomegalovirus · GO: gene ontology · LCMV: lymphocytic choriomeningitis virus · Listeria-OVA: OVA-expressing *Listeria monocytogenes* · SI: small intestine · SR1PR1: sphingosine-1-phosphate receptor · T_{CM}: central memory T cells · T_{EM}: effector memory T cells · T_{RM}: resident memory T cells

Full correspondence: Dr. Martijn A. Nolte, PhD, Department of Hematopoiesis, Sanquin Research, Plesmanlaan 125, 1066 CX Amsterdam, The Netherlands
e-mail: m.nolte@sanquin.nl

Additional correspondence: Maria F. Pascutti, PhD, Department of Hematopoiesis, Sanquin Research, Plesmanlaan 125, 1066 CX Amsterdam, The Netherlands
e-mail: f.pascutti@sanquin.nl

See accompanying Commentary:
<https://doi.org/10.1002/eji.201948208>

The peer review history for this article is available at
<https://publons.com/publon/10.1002/eji.201848003>

Received: 14/11/2018
Revised: 13/2/2019
Accepted: 18/3/2019
Accepted article online: 20/3/2019